CHANNEL ESTIMATION AND DETECTION FOR MULTI-INPUT MULTI-OUTPUT (MIMO) SYSTEMS

THI-NGA CAO

(B.Eng., HaNoi University of Technology)

A THESIS SUBMITTED

FOR THE DEGREE OF MASTER OF ENGINEERING

DEPARTMENT OF ELECTRICAL AND COMPUTER ENGINEERING

NATIONAL UNIVERSITY OF SINGAPORE

2006

SUMMARY

To meet the demand on very high data rates communication services, multiple transmitting and multiple receiving antennas have been proposed for modern wireless systems, where performance is limited by fading and noise. Most of the current studies on multiple-input multiple-output (MIMO) systems assume that the noise at receiving antennas are independent (white noise). In this dissertation, we focus on MIMO systems under colored noise, i.e., the noise at the receiving antennas are correlated.

Channel information estimation and data detection for MIMO systems under spatially colored noise are studied. We propose an algorithm for pilot symbol assisted joint estimation of the channel coefficients and noise covariance matrix. Our proposed method is applied in quasi-static flat fading, quasi-static frequency selective fading and flat fast fading. A strategy to apply Sphere Decoder in the spatially colored noise environment is also presented. This algorithm is used in the decoding stage of our proposed systems.

ACKNOWLEDGEMENTS

I would like to express my sincere gratitude and appreciation to A/P Ng Chun Sum, my supervisor, whose guidance, advice, patience are gratefully appreciated.

Special thanks also go to my colleague Mr. Zhang Qi for his fruitful and enlightening discussions on various topics in communication theory.

TABLE OF CONTENTS

LIST OF FIGURES

LIST OF SYMBOLS AND ABBREVIATIONS

$\mathbb{C}$	set of complex numbers
$\mathbb{R}$	set of real numbers
$\mathbb{Z}$	set of integer numbers
$\mathbb{Z}_Q$	set of integer belong to set of $[0, 1, 2, \cdots, Q-1]$
$\in$	is an element of
$\subset$	subset
$\emptyset$	empty set or null set
$\{x_n\}_{n=-\infty}^{+\infty}$	set of elements $\cdots, x_{-1}, x_0, x_1, \cdots$
e^x or $\exp\{x\}$	exponential function
$E\{\cdot\}$	(statistical) mean value or expected value
$\mathrm{Re}(\cdot)$	real part of a complex matrix/number
$\mathrm{Im}(\cdot)$	imaginary part of a complex matrix/number
$\log x$	natural logarithm of x
$\otimes$	Kronecker product
$x_1(t) * x_2(t)$	convolution of $x_1(t)$ and $x_2(t)$
$\lvert\boldsymbol{H}\rvert$	determinant of matrix $\boldsymbol{H}$
$\prod_{i=1}^{N}$	multiple product
$\sum_{i=1}^{N}$	multiple sum
$\lceil x \rceil$	ceiling function, the smallest integer greater than or equal x
$\lfloor x \rfloor$	floor function, the greatest integer less than or equal x
$\lceil x \rfloor$	nearest integer to x
$\sim$	distributed according to (statistics)
$\mathcal{CN}(m, \sigma^2)$	complex Gaussian random variable with mean of m and variance of σ^2
$\mathcal{CN}(\boldsymbol{m}, \boldsymbol{\Sigma})$	complex Gaussian random vector with mean of $\boldsymbol{m}$ and covariance matrix of $\boldsymbol{\Sigma}$
$(\cdot)^T$	transpose of a matrix/vector
$(\cdot)^{\mathcal{H}}$	conjugate transpose of a matrix/vector
$\boldsymbol{A}^\dagger$	pseudo-inverse of a matrix $\boldsymbol{A}$, $\boldsymbol{A}^\dagger = (\boldsymbol{A}^{\mathcal{H}}\boldsymbol{A})^{-1}\boldsymbol{A}^{\mathcal{H}}$
$\boldsymbol{0}_{m\times n}$	zero matrix of size $m \times n$
$\boldsymbol{I}_n$	identity matrix of size n
$\mathcal{C}$	QPSK symbols
AWGN	Additive White Gaussian Noise
BER	Bit-Error-Rate
CIR	Channel Impulse Response
DEML	Decouple Maximum Likelihood
FIR	Finite Impulse Response
IBI	Interblock Interference
i.i.d.	independent and identical distributed
ISI	Intersymbol Interference
LOS	Line-Of-Sight

MIMO	Multi-Input Multi-Output
MSE	Mean Square Error
PAM	Pulse Amplitude Modulation
QAM	Quadrature Amplitude Modulation
SD	Sphere Decoder
SNR	Signal-to-Noise Ratio

CHAPTER 1

INTRODUCTION

1.1 Motivations

Reliable communication over a wireless channel is a highly challenging problem due to the complex propagation medium. The major impairments of the wireless channel are fading and noise. Due to ground irregularities and typical wave propagation phenomena such as diffraction, scattering, and reflection, when a signal is launched into the wireless environment, it arrives at the receiver along a number of distinct paths, referred to as multipath phenomenon. Each of these paths has a distinct time-varying amplitude, phase and angle of arrival. These multipaths add up constructively or destructively at the receiver. Hence, the received signal can be distorted. The use of antenna arrays has been shown to be an effective technique for mitigating the effects of fading and noise [1, 2, 3]. Antenna arrays can be employed at the transmitter, or receiver, or both ends. With an antenna array at the receiver, fading can be reduced by diversity techniques, i.e., combining independently faded signals on different antennas that are separated sufficiently apart. If antennas receive independently faded signals, it is unlikely that all signals undergo deep fades, hence, at least one good signal can be received. To meet the requirement of very high data rates for modern wireless networks, multiple antennas at both the transmitter and receiver have been proposed [4, 5]. It was also proven that in a scattering rich environment where channel links between different transmitters and receivers fade independently, the Shannon's information capacity of a MIMO channel increases linearly with the smaller of the numbers of transmitting and receiving

antennas [6].

Most of the current studies on MIMO systems assume that the noise at the receiving antennas are independent (white noise). However, in MIMO systems, the noise may be dependent (colored noise) [7, 8]. In this dissertation, we focus on MIMO systems under colored noise. Therefore, besides channel coefficients, we have one more parameter to be concerned with, the noise covariance matrix. The ability to derive accurate information on channel properties from the received signal is thus more challenging compared to that of an additive white noise environment.

The design of suitable receiver structures that maximize system performance is another vital task in communication systems. The Maximum-Likelihood (ML) detector is well-known to be optimum but it has a major drawback of requiring high computational complexity. Recently, a method to solve the ML detection problems by using Sphere Decoders (SD), is proposed. Sphere decoders, in general, consisting of several variations, are algorithms derived from the closest lattice point problem which is widely investigated in lattice theory [9].

The SD was first applied to the ML detection problem in the early 90's [10] but gained main stream recognition with a later series of papers [11, 12]. To be specific, in [11], Viterbo and Boutros applied the SD to perform ML decoding of multidimensional constellations in a single transmit antenna and a single receive antenna system operating over an independent fading channel with perfect channel state information at the receiver. The decoder performs a bound distance search among the lattice points falling inside a sphere centered at the received point. In [12], Oussama Damen *et al.* successfully applied the

SD in uncoded and coded multi-antenna systems. The historical background as well as the current state of the art implementations of the algorithm have been recently covered in two semi-tutorial papers [13] and [14].

From the day of appearance, the SD algorithm has found many applications. Some examples include [12] which focuses on multi-antenna systems, [15] on the CDMA scenario, and [16] where the sphere decoder is extended to generate soft information required by concatenated coding schemes.

The complexity of SD is much lower than the directly implemented ML detection method, which needs to search through all possible candidates before making a decision. In [14], it is reported that the complexity of SD is polynomial in m (roughly, $O(m^3)$) where m is the number of variables to be decoded. The obtained performance of the SD algorithm is very promising. For example, in [12], the authors apply SD to solve the detection problem in a MIMO system. The results proved that SD can provide a huge performance improvement over the well-known sub-optimal V-BLAST detection algorithm. Furthermore, the complexity of SD method does not dependent on the number of signal points in the signal constellations. SD also outperforms other suboptimal detection scheme such as [17] in which authors applied the V-BLAST detection scheme but in a new lattice where the basis is transformed to get a better orthogonality among them in an operation called lattice reduction.

1.2 Contributions

In this dissertation, we consider MIMO systems under colored noise. We apply the decouple maximum-likelihood (DEML) estimator, which was first used in [18] to estimate the angle-of-arrival in antenna array systems, to estimate the

channel coefficients and noise covariance matrix for MIMO systems using pilot symbols. Our method can be applied in quasi-static flat fading, quasi-static frequency selective fading and flat fast fading.

A strategy for applying SD in colored noise environment is also introduced. The improvement in the proposed system bit-error-rate (BER) performance, using SD as the detection algorithm and using the information from the proposed channel estimation algorithm, over a classical detection method using perfect channel information is shown by simulation.

1.3 Organization of the dissertation

Chapter 2 presents the continuous time MIMO system where the discrete time MIMO system is developed.

Chapter 3 reviews the solution to the so-called closest lattice point problems for the case of infinite lattice. The two strategies to solve the closest lattice point problems, Pohst enumeration and Schnorr-Euchner enumeration, are presented. This chapter also give some examples to show that in many communication problems, the Maximum Likelihood (ML) problems can be translated into the closest lattice point problems but in finite lattices. The Sphere Decoder, the algorithm which solve the closest lattice point problems in finite lattice, is presented. Two Sphere Decoders are reviewed in the chapter, the first one relying on the Pohst enumeration and the second one on Schnorr-Euchner enumeration. The latter is noted to outperform the former in term of computational complexity. The Sphere Decoder so far deals with the case in which the noise at receivers of MIMO systems are independent. This chapter also give a strategy to deal with the case in which the noise components from receivers are correlated.

Chapter 4 presents the decouple maximum likelihood (DEML) estimator to estimate the channel information for MIMO systems under three types of fading: quasi-static flat fading, quasi-static frequency selective fading and flat fast fading. The DEML estimator relies on the pilot symbols placed at the beginning of the data frame to aid estimation of the channel coefficients and the noise covariance matrix at the receiver. The application of Sphere Decoding after obtaining the estimated channel information is presented.

Chapter 5 presents computer simulation results based on the theory developed in previous chapter.

Chapter 6 concludes the dissertation with the conclusion and recommendation for future works.

CHAPTER 2

BACKGROUND

In this chapter, we introduce the MIMO system model and the fading channel model that are considered in this dissertation.

2.1 Continuous time MIMO system model

We consider a MIMO communication system equipped with N_i transmitters and N_0 receivers. The system under consideration is depicted in Figure 2.1.

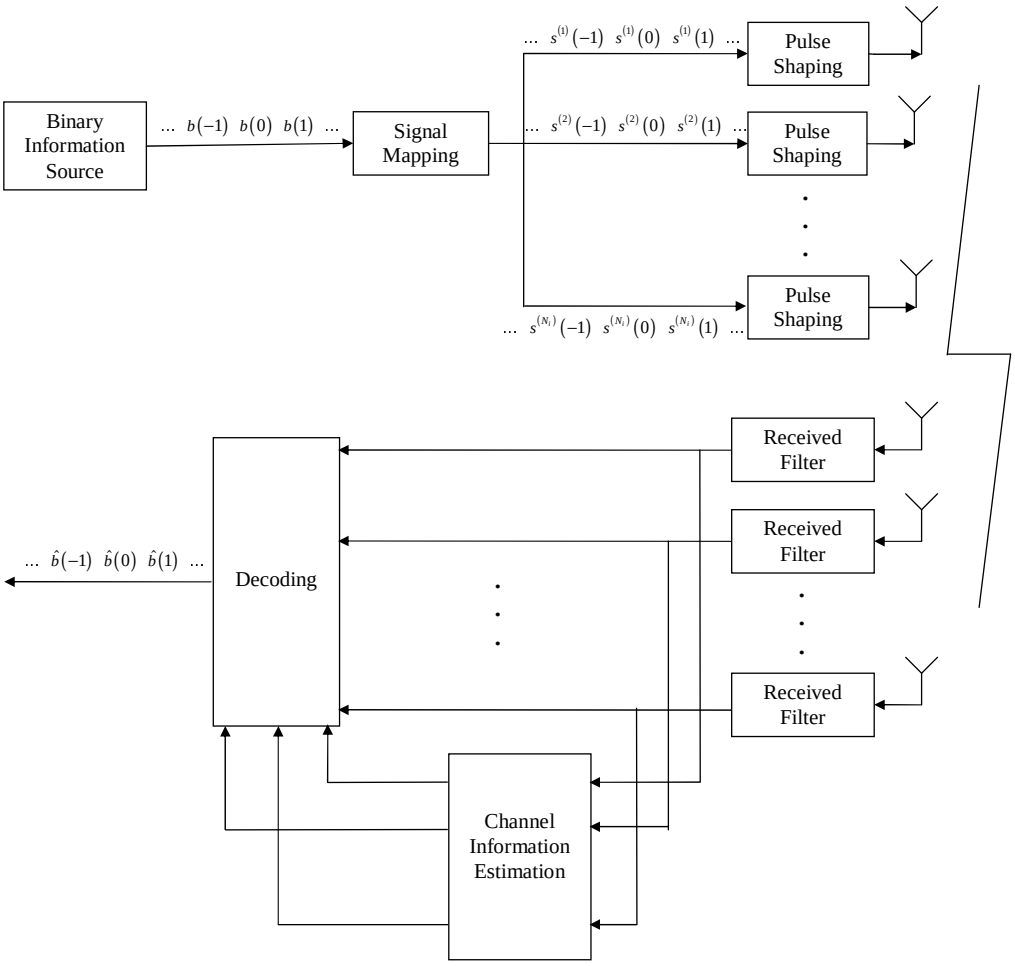

Figure 2.1: MIMO system model

2.1.1 Transmitter structure

Signal Mapping

In Figure 2.1, the binary information source generates the binary sequence $\{b(k)\}_{k=-\infty}^{+\infty}$ where k denotes the time index. This sequence is generated at the bit rate of $1/T_b$ and consists of independent identically distributed binary bits. The binary sequence is fed into the signal mapping block in which a bit or a combination of bits is mapped onto a symbol for transmission. The outputs of the signal mapping blocks are denoted as $\{s^{(i)}(k)\}_{k=-\infty}^{+\infty}$ where superscript $i, i = 1, 2, \cdots, N_i$ denotes the i^{th} transmitter. We consider a Gray-coded quadrature phase-shift keying (QPSK) in which $\{00, 01, 11, 10\}$ is mapped into $\{1+j, -1+j, -1-j, 1-j\}$ where $j = \sqrt{-1}$ (see Figure 2.2). After the signal mapping block, the symbol duration is $T = 2 \times T_b$.

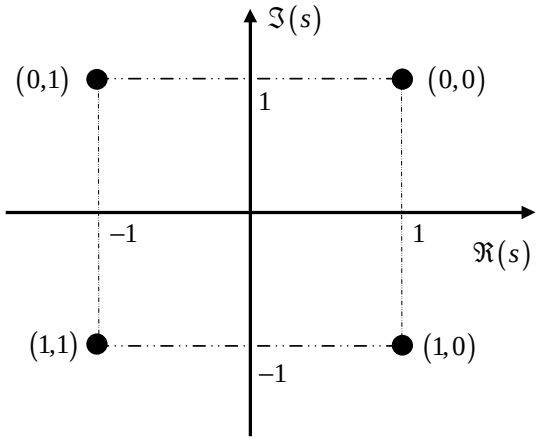

Figure 2.2: QPSK signal mapping illustration

Pulse shaping

The N_i parallel encoded sequences $\{s^{(i)}(k)\}_{k=-\infty}^{+\infty}$, $i = 1, 2, \cdots, N_i$ are sent to the pulse shaping blocks and transmitted simultaneously from N_i transmitters.

The pulse shaping blocks are illustrated in Figure 2.3 in which $p(t)$ denotes its impulse response.

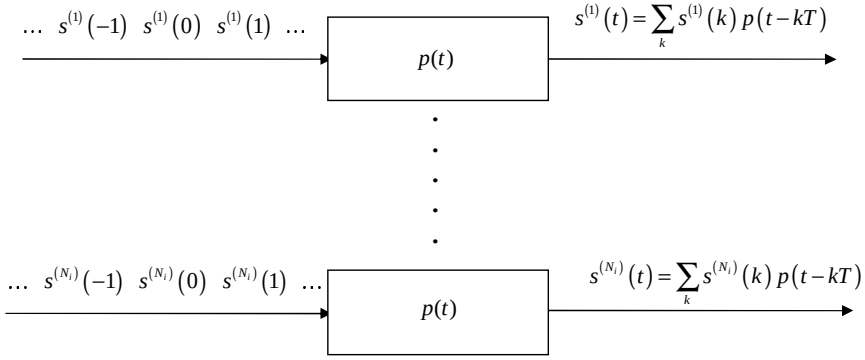

Figure 2.3: Spectrum shaping pulse blocks

The output of the i^{th} pulse shaping block (corresponding to i^{th} transmitter), which are sent to i^{th} transmitter for transmission, is written as

$$s^{(i)}(t) = \sum_k s^{(i)}(k)p(t - kT),\ \ i = 1, 2, \cdots, N_i. \tag{2.1}$$

2.1.2 Fading channel model

In urban area, *fading* is used to describe the rapid fluctuations of the amplitude and phase in the received signal. Because of the short propagation distance (or time), large-scale path loss may be ignored. Fading is caused by the interference between two or more versions of transmitted signal which arrive at receiver from different directions with different propagation delays. These multipath signals, which come from reflections from the ground and surrounding structures combine vectorially at the receiver, resulting in a received signal with randomly distributed amplitude, phase, angle of arrival. Depending on the relationship between signal parameters (such as bandwidth, symbol period, etc.) and the channel parameters (such as delay spread and Doppler spread), the transmitted

signal will experience different types of fading [19, 20].

If the channel has a constant gain and linear phase response over a bandwidth which is greater than the bandwidth of the transmitted signal, then the received signal undergoes *flat fading*. In flat fading, the multipath structure of the channel is such that the spectral characteristics of the transmitted signal are preserved at the receiver, i.e., all frequency components of the transmitted signal are affected in the same manner by the channel. Flat fading is mainly experienced in narrow-band systems where the bandwidth of transmitted signal is small compared with the coherence bandwidth of the channel, which is defined as the reciprocal of the multipath delay spread of the channel. On the other hand, if the channel possesses a constant gain and linear phase response over a bandwidth that is smaller than the bandwidth of the transmitted signal, then the channel introduces *frequency selective fading* on the received signal. Viewed in the frequency domain, certain frequency components in the received signal spectrum have greater gains than others. Frequency selective fading is mainly experienced in broad-band systems where the the bandwidth of the transmitted signal is larger than the coherence bandwidth of the channel. Frequency selective fading is manifested as time dispersion of the transmitted symbols within the channel and thus induces ISI.

Depending on how rapidly the transmitted baseband signal changes as compared to the rate of change of the channel, a channel maybe classified as *fast fading* or *slow fading* channel. In a fast fading channel, the channel impulse response changes rapidly within the symbol duration. That is, the coherence time of the channel is smaller than the symbol period of the transmitted signal. This causes frequency dispersion (also called time selective fading) due

to Doppler frequency shift, which leads to signal distortion. In a slow fading channel, however, the channel impulse response changes at a rate much slower than the transmitted baseband signal. Here, the coherence time is larger than the symbol period of the transmitted signal.

In this dissertation, we will consider three types of fading: flat, frequency selective and fast fading. The first two types of fading are considered in details in the Section 2.2. The last type is considered in Section 4.4.

2.1.3 Receiver structure

At the receiver end, which is depicted in Figure 2.4, the received signal $y^{(j)}(t)$ at the j^{th} receivers, $j = 1, 2, \cdots, N_0$, is a linear superposition of the N_i transmitted signals from N_i transmitters perturbed by fading and additive Gaussian noise.

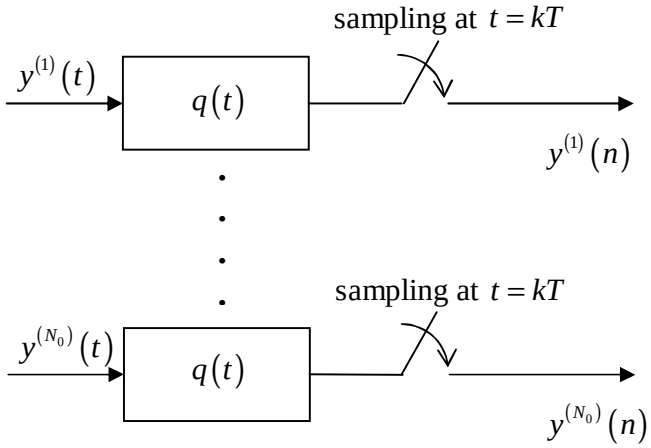

Figure 2.4: The structure of received filters

This received signal is sent to a received filter whose impulse response is $q(t)$ and the output of this filter is sampled with period of T. The obtained discrete-time signals from all N_0 receivers are used for the purpose of channel information estimation and detection.

2.2 Discrete-time MIMO system model

To develop the discrete-time MIMO system model for the model in Figure 2.1, we inspect only a link from i^{th} transmitter to j^{th} receiver in detail. This link is illustrated in Figure 2.5.

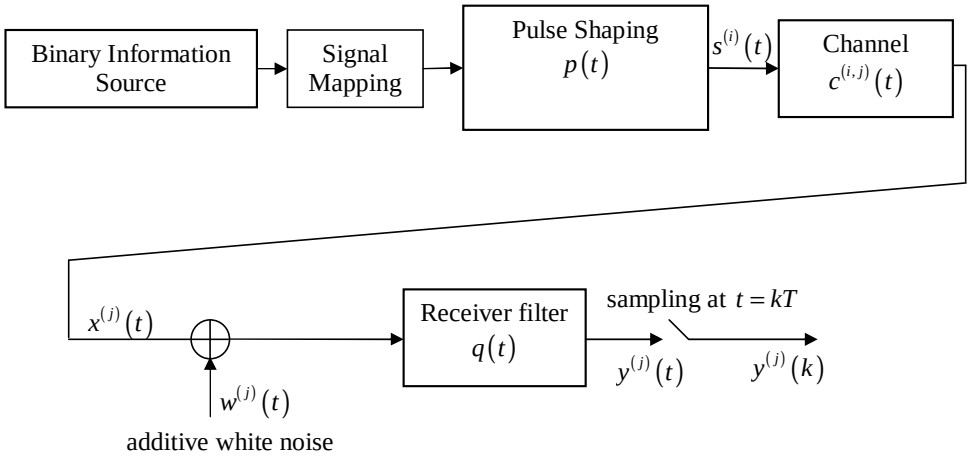

Figure 2.5: The link from i^{th} transmitter to j^{yh} receiver

Let $v(t) = p(t) * c^{(i,j)}(t)$. Then, $v(t)$ becomes the modified transmitter filter which includes the channel impulse response $c^{(i,j)}(t)$ of the link. The received signal $y^{(j)}(t)$ after receiver filtering is written as

$$\begin{aligned} y^{(j)}(t) &= \int (x^{(j)}(\tau) + w^{(j)}(\tau)) q(t-\tau) d\tau \\ &= \int q(t-\tau) \left(\sum_m s^{(i)}(m) v(\tau - mT) \right) d\tau + \int q(t-\tau) w(\tau) d\tau \\ &= \sum_m s^{(i)}(m) \int q(t-\tau) v(\tau - mT) d\tau + \int q(t-\tau) w(\tau) d\tau. \end{aligned} \quad (2.2)$$

The sampled signal of $y^{(j)}(t)$ is given by

$$\begin{aligned} y^{(j)}(k) &\triangleq y^{(j)}(t)\big|_{t=kT} = y^{(j)}(kT) \\ &= \sum_m s^{(i)}(m) \underbrace{\int q(kT-\tau) v(\tau - mT) d\tau}_{= q(t) * v(t)|_{t=(k-m)T}} + w^{(j)}(k) \end{aligned}$$

$$= \sum_m s^{(i)}(m)h^{(i,j)}(k-m) + w^{(j)}(k) \tag{2.3}$$

where $w^{(j)}(k) \triangleq \int q(nT-\tau)w(\tau)d\tau$ and $h^{(i,j)}(k-m) \triangleq q(t) * v(t)|_{t=(k-m)T}$.

The resulting received signal after sampling in the discrete time domain is given by

$$y^{(j)}(k) = \sum_m s^{(i)}(m)h^{(i,j)}(k-m) + w^{(j)}(k) = s^{(i)}(k) * h^{(i,j)}(k) + w^{(j)}(k) \tag{2.4}$$

where $h^{(i,j)}(k)$ is called the discrete time channel impulse response of the link.

From the investigation of one link, we generalized to our MIMO system with N_i transmitter and N_0 receivers to have the discrete-time MIMO system model which is depicted in Figure 2.6.

In this model, the noise $\{w^{(j)}(k)\}_{k=-\infty}^{+\infty}$ at the j^{th} receiver is assumed to consist of i.i.d. Gaussian random variables with zero mean and variance of σ_w^2 regardless of j. The noise at the N_0 receivers, in general, are assumed to be correlated.

The discrete-time channel impulse response of the link from i^{th} transmitter to j^{th} receiver $h^{(i,j)}(k),\ i = 1, 2, \cdots, N_i,\ j = 1, 2, \cdots, N_0$ depends on the type of fading under consideration.

If each link is a quasi-static frequency selective Rayleigh fading channel, $h^{(i,j)}(k)$ is described by a linear, time-invariant finite impulse response as [20]:

$$h^{(i,j)}(k) = \sum_{l=0}^{l=L} h_{i,j}(l)\delta(k-l);\quad i = 1, 2, \cdots, N_i,\ j = 1, 2, \cdots, N_0 \tag{2.5}$$

where $(L+1)$ is the length of the channel impulse response, $h_{i,j}(l)$ is a complex Gaussian random variable with zero mean and variance of σ_l^2, and $\delta(k)$ is the Kronecker's delta function.

If $L = 0$, then (2.5) specializes to the case of quasi-static flat fading where

$$h^{(i,j)}(k) = h_{i,j}(0)\delta(k). \tag{2.6}$$

In this case we may simplify the notation by writing $h_{i,j}(0) = h_{i,j}$ and $\sigma_0^2 = \sigma^2$.

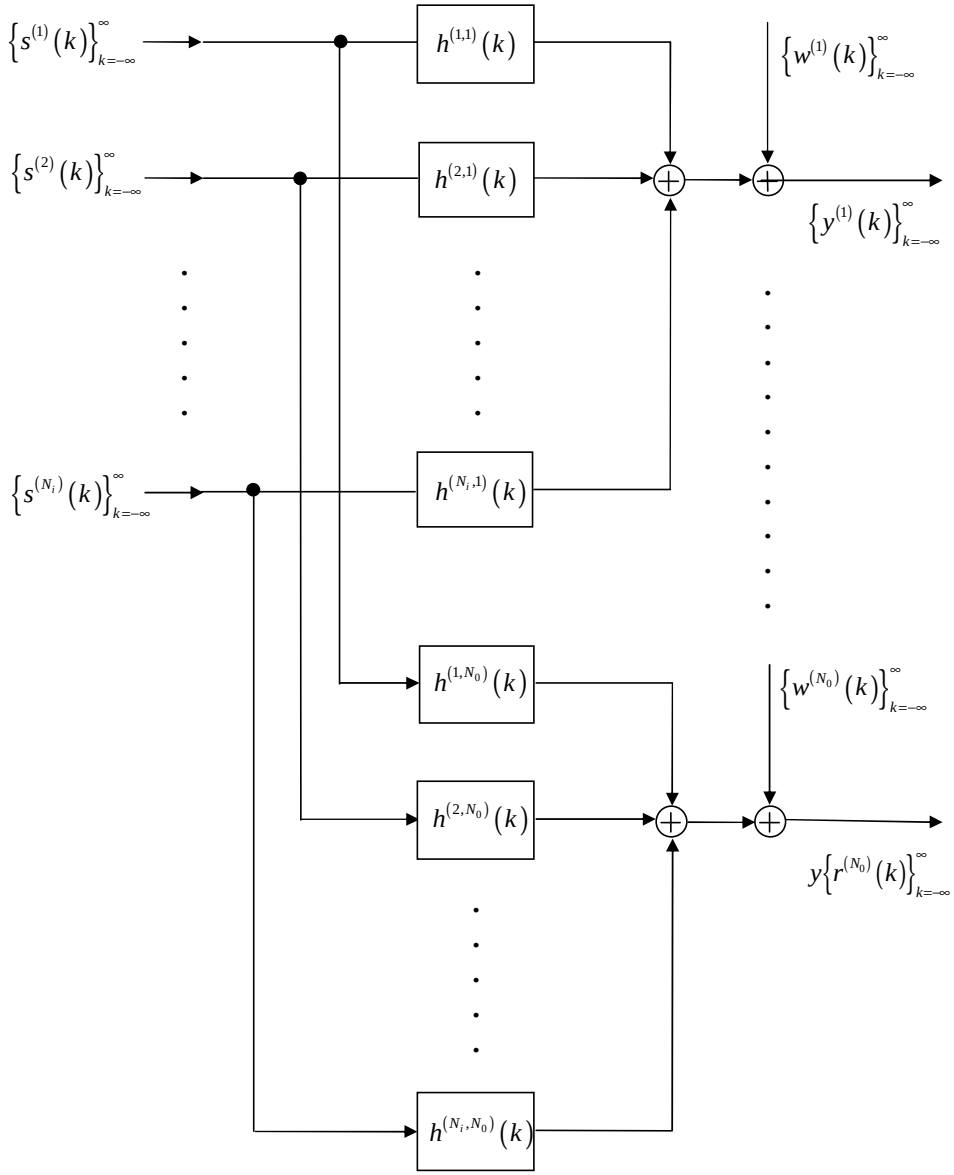

Figure 2.6: Discrete MIMO system model

2.3 Blocking and IBI Suppression for quasi-static frequency selective fading channels

For transmission over wireless dispersive media, the channel induced ISI is a major performance limiting factor. To mitigate such time-domain dispersive effect arising from frequency selectivity, it has been proven useful to transmit the information-bearing symbols in blocks [21]. To be specific, we once again consider the link from the i^{th} transmitter to j^{th} receiver in our MIMO system without the presence of other links. This link is modeled as a quasi-static frequency selective fading channel that has the length of CIR of $(L+1)$. We group the serial $s^{(i)}(k)$ into blocks of size $P >> L$ and correspondingly define the m^{th} transmitted block to be $\boldsymbol{s}^{(i)}(m) = [s^{(i)}(mP)\ s^{(i)}(mP+1)\ \cdots\ s^{(i)}(mP+P-1)]^T$ and the m^{th} received block as $\boldsymbol{y}^{(j)}(m) = [y^{(j)}(mP)\ y^{(j)}(mP+1)\ \cdots\ y^{(j)}(mP+P-1)]^T$. Using (2.4) and (2.5), we can relate transmit- with receive-block as (see Figure 2.7(a))

$$\boldsymbol{y}^{(j)}(m) = \boldsymbol{H}_0^{(i,j)}\boldsymbol{s}^{(i)}(m) + \boldsymbol{H}_1^{(i,j)}\boldsymbol{s}^{(i)}(m-1) + \boldsymbol{w}^{(j)}(m) \tag{2.7}$$

where $\boldsymbol{w}^{(j)}(m)$ is the corresponding noise vector, and the $P \times P$ matrices $\boldsymbol{H}_l^{(i,j)},\ l = 0, 1$ are defined as

$$\boldsymbol{H}_0^{(i,j)} = \begin{bmatrix} h_{i,j}(0) & 0 & 0 & \cdots & 0 \\ \vdots & h_{i,j}(0) & 0 & \cdots & 0 \\ h_{i,j}(L) & \cdots & \ddots & \cdots & \vdots \\ \vdots & \ddots & \cdots & \ddots & 0 \\ 0 & \cdots & h_{i,j}(L) & \cdots & h_{i,j}(0) \end{bmatrix}, \tag{2.8}$$

$$\boldsymbol{H}_1^{(i,j)} = \begin{bmatrix} 0 & \cdots & h_{i,j}(L) & \cdots & h_{i,j}(1) \\ \vdots & \ddots & 0 & \ddots & \vdots \\ 0 & \cdots & \ddots & \cdots & h_{i,j}(L) \\ \vdots & \vdots & \vdots & \ddots & \vdots \\ 0 & \cdots & 0 & \cdots & 0 \end{bmatrix}. \tag{2.9}$$

Due to the dispersive nature of the channel, IBI arises between successive blocks are described in $\boldsymbol{y}^{(j)}(m)$ in (2.7) dependent on both $\boldsymbol{s}^{(i)}(m)$ and $\boldsymbol{s}^{(i)}(m-1)$.

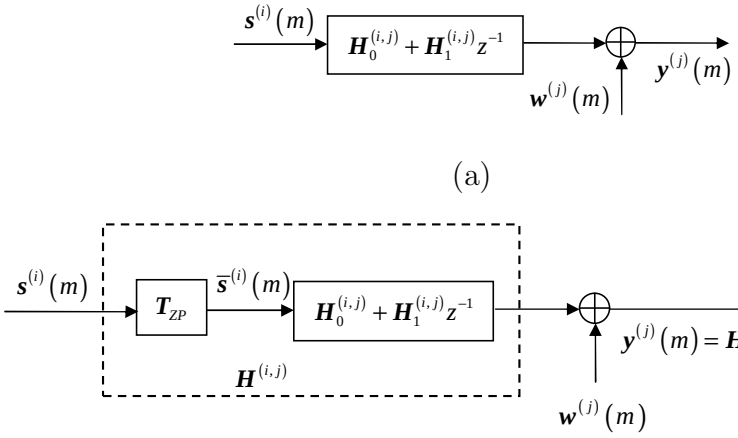

Figure 2.7: (a) Block with $P >> L$. (b) General block transmission with zero-padding

.

If the $\boldsymbol{s}^{(i)}(m)$ blocks are IBI free, then we can process them independently in an AWGN environment. To obtain IBI-free blocks, we need to introduce "guard symbols" in the transmitted block $\boldsymbol{s}^{(i)}(m)$. We start with an $N \times 1$ vector $\boldsymbol{s}^{(i)}(m)$ and create $\bar{\boldsymbol{s}}^{(i)}(m) = \boldsymbol{T}\boldsymbol{s}^{(i)}(m)$, where the guard-inserting matrix

$\boldsymbol{T}$ is $P \times N$, with $P = N + L$. We can write (2.7) as

$$\boldsymbol{y}^{(j)}(m) = \boldsymbol{H}_0^{(i,j)}\boldsymbol{T}\boldsymbol{s}^{(i)}(m) + \boldsymbol{H}_1^{(i,j)}\boldsymbol{T}\boldsymbol{s}^{(i)}(m-1) + \boldsymbol{w}^{(j)}(m) \tag{2.10}$$

We observe that P symbols are now used to transmit $N = P - L$ symbols. From (2.10), if $\boldsymbol{T}$ is chosen such that $\boldsymbol{H}_1^{(i,j)}\boldsymbol{T} = \boldsymbol{0}_{P\times N}$, then IBI disappears. This corresponds to zero-padded (ZP) block transmission. In our matrix model, it amounts to setting the last L rows of $\boldsymbol{T}$ to zero, i.e., $\boldsymbol{T} = \boldsymbol{T}_{ZP} = [\boldsymbol{I}_N^T \ \boldsymbol{0}_{L\times N}^T]^T$ where $\boldsymbol{I}_N$ is the identity matrix of size N and $\boldsymbol{0}_{L\times N}$ is a zero matrix of size $L \times N$. Since only the last L columns of $\boldsymbol{H}_1^{(i,j)}$ in (2.7) are nonzero, it can be easily verified that $\boldsymbol{H}_1^{(i,j)}\boldsymbol{T}_{ZP} = \boldsymbol{0}_{P\times N}$ because right-multiplying with $\boldsymbol{T}_{ZP}$ is equivalent to discarding L columns on the right.

Forming the $P \times N$ matrix

$$\boldsymbol{H}^{(i,j)} = \boldsymbol{H}_0^{(i,j)}\boldsymbol{T}_{ZP} = \begin{bmatrix} h_{i,j}(0) & 0 & \cdots & 0 \\ \vdots & h_{i,j}(0) & \cdots & 0 \\ h_{i,j}(L) & \ddots & \ddots & \vdots \\ \vdots & \ddots & \ddots & h_{i,j}(0) \\ \vdots & \ddots & \ddots & \vdots \\ 0 & 0 & \cdots & h_{i,j}(L) \end{bmatrix}$$

from the first N columns of matrix $\boldsymbol{H}_0^{(i,j)}$, we can write the received block $\boldsymbol{y}^{(j)}(m)$ as

$$\boldsymbol{y}^{(j)}(m) = \boldsymbol{H}^{(i,j)}\boldsymbol{s}(m) + \boldsymbol{w}^{(j)}(m). \tag{2.11}$$

Hence, before the symbols are fed into the pulse shaping blocks for transmission, the symbols are grouped to form a block and then zero-padded with L numbers of 0 symbols to avoid IBI caused by frequency selective fading.

2.4 Summary

In this chapter, a general continuous time MIMO system model is introduced together with a brief review of fading channel models. We then develop the general discrete-time MIMO system model for purpose of our study. The zero-padding method to avoid IBI for systems operating in frequency selective fading channels is also addressed.

CHAPTER 3

SPHERE DECODER

3.1 Introduction

In this chapter we shall be concerned with the following so-called *integer least-squares problem*

$$\min_{\mathbf{s}\in\mathbb{Z}^m} \|\mathbf{y}-\mathbf{H}\mathbf{s}\|^2 \tag{3.1}$$

where $\mathbf{y}\in\mathbb{R}^n, \mathbf{H}\in\mathbb{R}^{n\times m}$, in which $\mathbb{R}$ denotes the set of real numbers and $\mathbb{Z}^m$ denotes the $m-$dimensional integer lattice, i.e., $\mathbf{s}$ is an $m-$dimensional vector with integer components. In practical communication problems, the search space is a finite subset, $\mathcal{D}$, of the infinite lattice $\mathbb{Z}^m$, where we have

$$\min_{\mathbf{s}\in\mathcal{D}\subset\mathbb{Z}^m} \|\mathbf{y}-\mathbf{H}\mathbf{s}\|^2. \tag{3.2}$$

The integer least-squares problem has a simple geometric interpretation. As the components of $\mathbf{s}$ take on integer values, $\mathbf{s}$ spans the "rectangular" $m-$dimensional lattice, $\mathbb{Z}^m$. However, for any given *lattice-generating matrix* $\mathbf{H}$, the $n-$dimensional vector $\mathbf{Hs}$ spans a "skewed" lattice. When $n>m$, this skewed lattice lies in an $m-$dimensional subspace of $\mathbb{R}^n$. Therefore, given the skewed lattice $\mathbf{Hs}$, and given a vector $\mathbf{y}\in\mathbb{R}^n$, the integer least-squares problem is to find the "closest" lattice point (in the Euclidean sense) to $\mathbf{y}$ [14] . This idea is illustrated in Figure 3.1

Compared to the standard least-squares problem where the unknown vector $\mathbf{s}$ is an arbitrary vector in $\mathbb{R}^m$, and the solution is obtained by using a simple pseudo-inverse, it is much more difficult to find the solution to problems (3.1) and (3.2). It is well-known that problems (3.1) and (3.2) are, for a general $\mathbf{H}$,

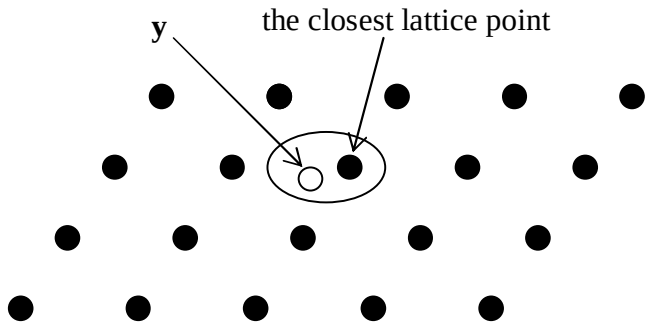

Figure 3.1: Geometrical interpretation of the integer least-squares problem.

NP-hard [22]. In [23], Pohst proposed an efficient strategy for enumerating all the lattice points within a sphere of certain radius. Although Pohst's enumeration has the worst case complexity that is exponential in m, it has been widely used due to its efficiency in many useful scenarios.

The Pohst enumeration strategy was first introduced in digital communications by Viterbo and Biglieri [10]. In [11], Viterbo and Boutros applied it to the ML detection of multidimensional constellations transmitted over a single antenna in fading channels where a flowchart of a specific implementation was given.

In the following sections of this chapter we shall investigate the sphere decoders through the Pohst and Schnorr-Euchner enumerations. Afterward, applications of the sphere decoders in communications problems are reviewed.

3.2 The Pohst and Schnorr-Euchner Enumerations

We come back to problem of (3.1)

$$\hat{\mathbf{s}} = \min_{\mathbf{s}\in\mathbb{Z}^m} \|\mathbf{y} - \mathbf{H}\mathbf{s}\|^2.$$

The set $\Lambda = \{\mathbf{H}\mathbf{s} : \mathbf{s} \in \mathbb{Z}^m\}$ is an $m-$dimensional lattice in $\mathbb{R}^n$.

Let C_0 be the squared radius of an $n-$dimensional sphere $\mathcal{S}(\mathbf{y}, \sqrt{C_0})$ centered at $\mathbf{y}$. We wish to produce a list of all points of $\Lambda \cap \mathcal{S}(\mathbf{y}, \sqrt{C_0})$. By performing the Gram-Schmidt orthonormalization of the columns of $\mathbf{H}$ (equivalently, by applying QR decomposition on $\mathbf{H}$), we have

$$\mathbf{H} = [\mathbf{Q}\ \mathbf{Q}^{'}] \begin{bmatrix} \mathbf{R} \\ \mathbf{0}_{m\times n} \end{bmatrix} \tag{3.3}$$

where $\mathbf{R}$ is an $m \times m$ upper triangular matrix, $\mathbf{Q}$ (respectively, $\mathbf{Q}^{'}$) is an $n \times m$ (respectively, $n \times (n-m)$) unitary matrix. The condition $\mathbf{Hs} \in \mathcal{S}(\mathbf{y}, \sqrt{C_0})$ can be written as [14]

$$\begin{aligned}
\|\mathbf{y} - \mathbf{Hs}\|^2 &\leq C_0, \\
\left\| [\mathbf{Q}\ \mathbf{Q}^{'}]^T\mathbf{y} - [\mathbf{Q}\ \mathbf{Q}^{'}]^T[\mathbf{Q}\ \mathbf{Q}^{'}] \begin{bmatrix} \mathbf{R} \\ \mathbf{0}_{m\times n} \end{bmatrix} \mathbf{s} \right\|^2 &\leq C_0, \\
\left\| [\mathbf{Q}\ \mathbf{Q}^{'}]^T\mathbf{y} - \begin{bmatrix} \mathbf{R} \\ \mathbf{0}_{m\times n} \end{bmatrix} \mathbf{s} \right\|^2 &\leq C_0, \\
\left\| \mathbf{Q}^T\mathbf{y} - \mathbf{Rs} \right\|^2 &\leq C_0 - \|(\mathbf{Q}^{'})^T\mathbf{y}\|, \\
\|\mathbf{y}^{'} - \mathbf{Rs}\|^2 &\leq C_0^{'},
\end{aligned} \tag{3.4}$$

where $\mathbf{y}^{'} = \mathbf{Q}^T\mathbf{y}$ and $C_0^{'} = C_0 - \|(\mathbf{Q}^{'})^T\mathbf{y}\|^2$. Due to the upper triangular form of $\mathbf{R}$, (3.4) can be expressed as

$$\left\| \begin{bmatrix} \mathrm{y}_1^{'} \\ \vdots \\ \mathrm{y}_{m-1}^{'} \\ \mathrm{y}_m^{'} \end{bmatrix} - \begin{bmatrix} \mathrm{r}_{1,1} & \cdots & \cdots & \mathrm{r}_{1,m} \\ \vdots & \ddots & \ddots & \vdots \\ 0 & \cdots & \mathrm{r}_{m-1,m-1} & \mathrm{r}_{m-1,m} \\ 0 & \cdots & 0 & \mathrm{r}_{m,m} \end{bmatrix} \times \begin{bmatrix} \mathrm{s}_1 \\ \vdots \\ \mathrm{s}_{m-1} \\ \mathrm{s}_m \end{bmatrix} \right\|^2 \leq C_0^{'},$$

$$\left\| \begin{bmatrix} \mathrm{y}_1^{'} - \sum_{l=1}^{m} \mathrm{r}_{1,l}\mathrm{s}_l \\ \vdots \\ \mathrm{y}_{m-1}^{'} - \sum_{l=m-1}^{m} \mathrm{r}_{m-1,l}\mathrm{s}_l \\ \mathrm{y}_m^{'} - \sum_{l=m}^{m} \mathrm{r}_{m,l}\mathrm{s}_l \end{bmatrix} \right\|^2 \leq C_0^{'}. \quad (3.5)$$

The above inequality implies a set of conditions

$$\sum_{j=i}^{m} \left| \mathrm{y}_j^{'} - \sum_{l=j}^{m} \mathrm{r}_{j,l}\mathrm{s}_l \right|^2 \leq C_0^{'}, \quad i = 1, 2, \cdots, m. \quad (3.6)$$

For example, if $i = m$, we have

$$|\mathrm{y}_m^{'} - \mathrm{r}_{m,m}\mathrm{s}_m|^2 \leq C_0^{'}. \quad (3.7)$$

This condition is equivalent to s_m belonging to the interval

$$\left\lceil \frac{1}{\mathrm{r}_{m,m}} \left(\mathrm{y}_m^{'} - \sqrt{C_0^{'}} \right) \right\rceil \leq \mathrm{s}_m \leq \left\lfloor \frac{1}{\mathrm{r}_{m,m}} \left(\mathrm{y}_m^{'} + \sqrt{C_0^{'}} \right) \right\rfloor. \quad (3.8)$$

For every s_m satisfying (3.8), the condition on s_{m-1} is

$$|\mathrm{y}_{m-1}^{'} - \mathrm{r}_{m-1,m-1}\mathrm{s}_{m-1} - \mathrm{r}_{m-1,m}\mathrm{s}_m|^2 + |\mathrm{y}_m^{'} - \mathrm{r}_{m,m}\mathrm{s}_m|^2 \leq C_0^{'} \quad (3.9)$$

which leads to s_{m-1} belonging to the interval

$$\left\lceil \frac{1}{\mathrm{r}_{m-1,m-1}} \left(\mathrm{y}_{m-1}^{'} - \mathrm{r}_{m-1,m}\mathrm{s}_m - \sqrt{C_0^{'} - |\mathrm{y}_m^{'} - \mathrm{r}_{m,m}\mathrm{s}_m|^2} \right) \right\rceil \leq \mathrm{s}_{m-1} \leq \left\lfloor \frac{1}{\mathrm{r}_{m-1,m-1}} \left(\mathrm{y}_{m-1}^{'} - \mathrm{r}_{m-1,m}\mathrm{s}_m + \sqrt{C_0^{'} - |\mathrm{y}_m^{'} - \mathrm{r}_{m,m}\mathrm{s}_m|^2} \right) \right\rfloor. \quad (3.10)$$

One can continue in a similar fashion for s_{m-2}, and so on until s_1. In conclusion, by considering (3.6) in the order from m to 1 (akin to back-substitution in the solution of a linear upper triangular system), we obtain the set of *admissible values* of each symbol s_i for given values of symbols $\mathrm{s}_{i+1}, \cdots, \mathrm{s}_m$. More explicitly, let $\mathbf{s}_l = [\mathrm{s}_l, \mathrm{s}_{l+1}, \cdots, \mathrm{s}_m]^T$ denote the last $m - l + 1$ components of

the vector $\mathbf{s}$. For a fixed $\mathbf{s}_{i+1}$, the component s_i can take on values in the range $\mathcal{R}_i(\mathbf{s}_{i+1}) = [L_i(\mathbf{s}_{i+1}), U_i(\mathbf{s}_{i+1})]$ where

$$L_i(\mathbf{s}_{i+1}) = \left\lceil \frac{1}{\mathrm{r}_{i,i}} \left(\mathrm{y}_i^{'} - \sum_{j=i+1}^{m} \mathrm{r}_{i,j}\mathrm{s}_j - \sqrt{C_0^{'} - \sum_{j=i+1}^{m} |\mathrm{y}_j^{'} - \sum_{l=j}^{m} \mathrm{r}_{j,l}\mathrm{s}_l|^2} \right) \right\rceil ,$$
$$U_i(\mathbf{s}_{i+1}) = \left\lfloor \frac{1}{\mathrm{r}_{i,i}} \left(\mathrm{y}_i^{'} - \sum_{j=i+1}^{m} \mathrm{r}_{i,j}\mathrm{s}_j + \sqrt{C_0^{'} - \sum_{j=i+1}^{m} |\mathrm{y}_j^{'} - \sum_{l=j}^{m} \mathrm{r}_{j,l}\mathrm{s}_l|^2} \right) \right\rfloor . \tag{3.11}$$

If $\sum_{j=i+1}^{m} |\mathrm{y}_j^{'} - \sum_{l=j}^{m} \mathrm{r}_{j,l}\mathrm{s}_l|^2 > C_0^{'}$ or $L_i(\mathbf{s}_{i+1}) > U_i(\mathbf{s}_{i+1})$, then $\mathcal{R}_i(\mathbf{s}_{i+1}) = \emptyset$. In this case, there is no value of s_i satisfying the inequalities (3.6) and the points corresponding to this choice of $\mathbf{s}_{i+1}$ do not belong to the sphere $\mathcal{S}(\mathbf{y}, \sqrt{C_0})$.

Pohst enumeration consists of spanning at each level i the admissible interval $\mathcal{R}_i(\mathbf{s}_{i+1})$, starting from level $i = m$ and climbing "up" to level $i = m-1, m-2, \cdots, 1$. At each level, the interval $\mathcal{R}_i(\mathbf{s}_{i+1})$ is determined by the current values of the variables at lower levels (corresponding to higher indexes). If $\mathcal{R}_1(\mathbf{s}_2)$ is nonempty, the vector $\mathbf{s} = [\mathrm{s}_1 \ \mathbf{s}_2^T]^T$, for all $\mathrm{s}_1 \in \mathcal{R}_1(\mathbf{s}_2)$, yield lattice points $\mathbf{Hs} \in \mathcal{S}(\mathbf{y}, \sqrt{C_0})$. The squared Euclidean distances between such points and $\mathbf{y}$ are given by

$$d^2(\mathbf{y}, \mathbf{Hs}) = \sum_{j=1}^{m} |\mathrm{y}_j^{'} - \sum_{l=j}^{m} \mathrm{r}_{j,l}\mathrm{s}_l|^2.$$

The algorithm outputs the point $\hat{\mathbf{s}}$ for which this distance is minimum. If, after spanning the interval $\mathcal{R}_m$ corresponding to s_m, no point in the sphere is found, the sphere is declared empty and the search fails. In this case, the search squared radius C_0 must be increased and the search is restarted with the new squared radius.

Pohst enumeration is based on the so-called *natural spanning* of the interval $\mathcal{R}_i(\mathbf{s}_{i+1})$ at each level i, i.e., s_i takes on values in the order $L_i(\mathbf{s}_{i+1}), L_i(\mathbf{s}_{i+1}) +$

$1, \cdots, U_i(\mathbf{s}_{i+1}) - 1, U_i(\mathbf{s}_{i+1})$. Schnorr-Euchner enumeration is a variation of the Pohst strategy where the intervals are spanned in a zig-zag order, starting from the middle point

$$\mathcal{M}_i(\mathbf{s}_{i+1}) = \left\lfloor \frac{1}{\mathrm{r}_{i,i}} \left(\mathrm{y}_i^{'} - \sum_{j=i+1}^{m} \mathrm{r}_{i,j}\mathrm{s}_j \right) \right\rceil . \tag{3.12}$$

Hence, the Schnorr-Euchner enumeration will produce at each level i the ordered sequence of values

$$\mathrm{s}_i \in \{\mathcal{M}_i(\mathbf{s}_{i+1}), \mathcal{M}_i(\mathbf{s}_{i+1}) + 1, \mathcal{M}_i(\mathbf{s}_{i+1}) - 1, \\ \mathcal{M}_i(\mathbf{s}_{i+1}) + 2, \mathcal{M}_i(\mathbf{s}_{i+1}) - 2, \cdots\} \cap \mathcal{R}_i(\mathbf{s}_{i+1})$$

if

$$\mathrm{y}_i^{'} - \sum_{j=i+1}^{m} \mathrm{r}_{i,j}\mathrm{s}_j - \mathrm{r}_{i,i}\mathcal{M}_i(\mathbf{s}_{i+1}) \geq 0$$

or the ordered sequence of value

$$\mathrm{s}_i \in \{\mathcal{M}_i(\mathbf{s}_{i+1}), \mathcal{M}_i(\mathbf{s}_{i+1}) - 1, \mathcal{M}_i(\mathbf{s}_{i+1}) + 1, \\ \mathcal{M}_i(\mathbf{s}_{i+1}) - 2, \mathcal{M}_i(\mathbf{s}_{i+1}) + 2, \cdots\} \cap \mathcal{R}_i(\mathbf{s}_{i+1})$$

if

$$\mathrm{y}_i^{'} - \sum_{j=i+1}^{m} \mathrm{r}_{i,j}\mathrm{s}_j - \mathrm{r}_{i,i}\mathcal{M}_i(\mathbf{s}_{i+1}) < 0.$$

Similar to the Pohst enumeration, when a given value of s_i results in a point segment $\mathbf{s}_{i+1}$ outside the sphere, the next value of s_{i+1} (at level $i+1$) is produced.

3.3 Sphere Decoders

In the previous section, we investigated the closest point search problem in infinite lattices. However, in communication applications, we deal with finite

lattices. In particular, the vector $\mathbf{s}$ does not belong to infinite lattice $\mathbb{Z}^m$ but a subset, $\mathbb{Z}_Q^m$, of it where $\mathbb{Z}_Q = \{0, 1, \cdots, Q-1\}$ (this point is addressed in details in the next section). Hence, our problem is

$$\hat{\mathbf{s}} = \arg \min_{\mathbf{s} \in \mathbb{Z}_Q^m} \|\mathbf{y} - \mathbf{H}\mathbf{s}\|^2. \tag{3.13}$$

Probably, the most immediate application of the Pohst enumeration to solve (3.13) is summarized in Algorithm 1

Algorithm 1

Step 1. Fix C_0

Step 2. Apply the Pohst enumeration with the interval boundaries modified as

$$L_i(\mathbf{s}_{i+1}) = \max \left\{ 0, \left\lceil \frac{1}{\mathrm{r}_{i,i}} \left(\mathrm{y}_i^{'} - \sum_{j=i+1}^{m} \mathrm{r}_{i,j}\mathrm{s}_j - \sqrt{C_0^{'} - \sum_{j=i+1}^{m} |\mathrm{y}_j^{'} - \sum_{l=j}^{m} \mathrm{r}_{j,l}\mathrm{s}_l|^2} \right) \right\rceil \right\}$$

$$U_i(\mathbf{s}_{i+1}) = \min \left\{ Q-1, \left\lfloor \frac{1}{\mathrm{r}_{i,i}} \left(\mathrm{y}_i^{'} - \sum_{j=i+1}^{m} \mathrm{r}_{i,j}\mathrm{s}_j + \sqrt{C_0^{'} - \sum_{j=i+1}^{m} |\mathrm{y}_j^{'} - \sum_{l=j}^{m} \mathrm{r}_{j,l}\mathrm{s}_l|^2} \right) \right\rfloor \right\}$$

and obtain the list of all vector $\mathbf{s} \in \mathbb{Z}_Q^m$ such that $\mathbf{H}\mathbf{s} \in \mathcal{S}(\mathbf{y}, C_0)$.

Step 3. If the list is nonempty, output the point achieving minimum distance (i.e., the ML decision). Otherwise, increasing C_0 and search again.

An improved version of the above algorithm, the Viterbo and Boutros algorithm (VB algorithm) [11], allowed C_0 to change adaptively along the search: that is as soon as a vector $\mathbf{s} \in \mathbb{Z}_Q^m$ is found such that $\mathbf{H}\mathbf{s} \in \mathcal{S}(\mathbf{y}, \sqrt{C_0})$, then C_0 is updated as

$$C_0 \longleftarrow d^2(\mathbf{y}, \mathbf{H}\mathbf{s})$$

and the search is restarted in the new sphere with the smaller radius. The drawback of this approach is that the VB algorithm may respan values of s_i for some level $i, 1 < i \leq m$, that have been already been spanned in the previous sphere.

In [14], an algorithm is presented to overcome the respanning of already spanned point segments. Also in [14], an algorithm that utilizes the Schnorr-Euchner strategy, which is proven to be more robust than the Pohst-based algorithms, is summarised in Algorithm 2.

3.4 Application of Sphere Decoder in Communications Problems

In many communication problems, the received signal is given by a linear combination of data symbols corrupted by additive noise. The input-output relationship describing such systems can be put in the form as follows:

$$\boldsymbol{y} = \tilde{\boldsymbol{H}}\boldsymbol{s} + \boldsymbol{w} \tag{3.14}$$

where $\boldsymbol{s}$, $\boldsymbol{y}$, $\boldsymbol{w}$ denote the system input, output and noise signals, respectively and $\tilde{\boldsymbol{H}}$ is a matrix representing the system linear mapping. The noise components are i.i.d. zero-mean complex Gaussian random variables with a common variance.

The specific structures of (3.14) are explained in the following two examples.

- *Example 1*

Suppose, we consider a flat fading MIMO system having N_i transmitters

Algorithm 2 Input $C_0^{'}$, $\mathbf{y}^{'}$, $\mathbf{R}$ Output $\hat{\mathbf{s}}$

Step 1. (Initialization) Set $i := m, T_m := 0, \xi_m := 0$ and $d_c := C_0^{'}$ (current sphere radius)

Step 2. Set $\mathrm{s}_i := \lfloor (\mathrm{y}_i^{'} - \xi_i)/\mathrm{r}_{i,i} \rceil$ and $\Delta_i := \mathrm{sign}(\mathrm{y}_i^{'} - \xi_i - \mathrm{r}_{i,i}\mathrm{s}_i)$

Step 3. (Main step)

If $d_c < T_i + |\mathrm{y}_i^{'} - \xi_i - \mathrm{r}_{i,i}\mathrm{s}_i|$

Go to Step 4 (i.e., we are outside the sphere)

Else if $\mathrm{s}_i \notin [0, Q-1]$

Go to Step 6 (i.e., we are inside the sphere but outside the signal set boundaries)

Else (i.e., we are inside the sphere and signal set boundaries)

if $i > 1$

$\xi_{i-1} := \sum_{j=i}^{m} \mathrm{r}_{i-1,j}\mathrm{s}_j; \quad T_{i-1} := T_i + |\mathrm{y}_i^{'} - \xi_i - \mathrm{r}_{i,i}\mathrm{s}_i|^2$

$i := i - 1$

Go to Step 2

else (i.e., $i = 1$)

Go to Step 5

Step 4.

If $i = m$

Terminate

Else

Set $i := i + 1$. Go to Step 6

Step5. (A valid point is found)

Let $d_c := T_1 + |\mathrm{y}_1^{'} - \xi_1 - \mathrm{r}_{1,1}\mathrm{s}_1|^2$. Save $\hat{\mathbf{s}} := \mathbf{s}$. Let $i := i + 1$ and go to Step 6.

Step 6. (Schnorr-Euchner enumeration of level i)

Let $\mathrm{s}_i := \mathrm{s}_i + \Delta_i$

$\Delta_i := -\Delta_i - \mathrm{sign}(\Delta_i)$

Go to Step 3.

and N_0 receivers that is illustrated in Figure 3.2. We assume that the

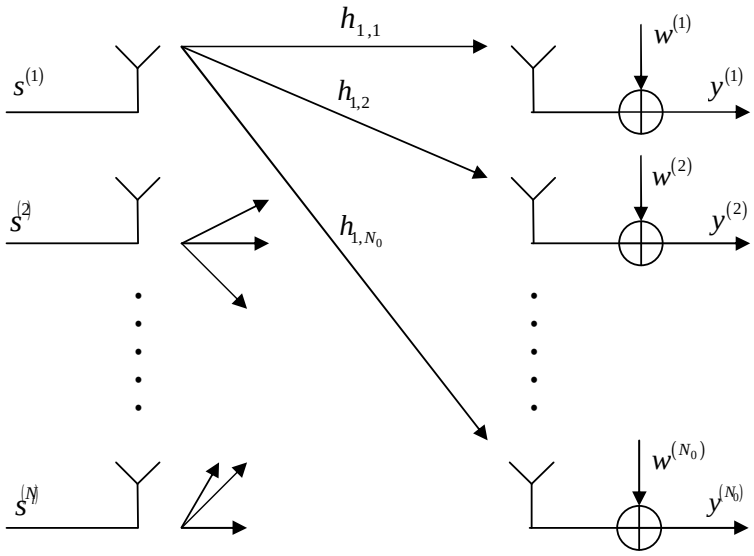

Figure 3.2: Multiple antenna system

environment between transmitters and receivers is quasi-static, i.e., the channel coefficients remain unchanged over one or several symbol periods. If that is the case, the input-output relationship can be written at any time instant as

$$\underbrace{\begin{bmatrix} y^{(1)} \\ \vdots \\ y^{(N_0)} \end{bmatrix}}_{\boldsymbol{y}} = \underbrace{\begin{bmatrix} h_{1,1} & h_{2,1} & \cdots & h_{N_i,1} \\ \vdots & \vdots & \vdots & \vdots \\ h_{1,N_0} & h_{2,N_0} & \cdots & h_{N_i,N_0} \end{bmatrix}}_{\tilde{\boldsymbol{H}}} \times \underbrace{\begin{bmatrix} s^{(1)} \\ \vdots \\ s^{(N_i)} \end{bmatrix}}_{\boldsymbol{s}} + \underbrace{\begin{bmatrix} w^{(1)} \\ \vdots \\ w^{(N_0)} \end{bmatrix}}_{\boldsymbol{w}} \tag{3.15}$$

where $\tilde{\boldsymbol{H}} \in \mathbb{C}^{N_0 \times N_i}$ is the known channel matrix, and $\boldsymbol{w} \in \mathbb{C}^{N_0 \times 1}$ is the additive white Gaussian noise vector consisting of i.i.d. complex Gaussian random variables with zero mean and variance of σ^2, i.e., $\boldsymbol{w} \sim \mathcal{CN}\left(\boldsymbol{0}, \sigma^2 \boldsymbol{I}_{N_0}\right)$ (white noise).

- *Example 2*

Suppose we consider a system consisting of one transmitter and one receiver working in a frequency selective FIR fading channel modeled in Figure 3.3.

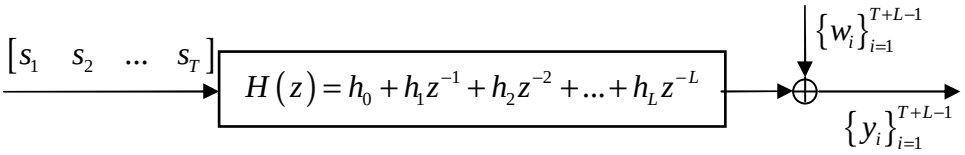

Figure 3.3: Frequency selective FIR channel

Here, the received signals can be written as

$$\underbrace{\begin{bmatrix} y_1 \\ y_2 \\ \vdots \\ \vdots \\ \vdots \\ y_{T+L} \\ y_{T+L+1} \end{bmatrix}}_{\boldsymbol{y}} = \underbrace{\begin{bmatrix} h_0 & & & \\ h_1 & h_0 & & \\ \vdots & \ddots & \ddots & \\ h_L & \vdots & \ddots & h_0 \\ & h_L & \vdots & h_1 \\ & & \ddots & \vdots \\ & & & h_L \end{bmatrix}}_{\tilde{\boldsymbol{H}}} \times \underbrace{\begin{bmatrix} s_1 \\ s_2 \\ \vdots \\ \vdots \\ s_T \end{bmatrix}}_{\boldsymbol{s}} + \underbrace{\begin{bmatrix} w_1 \\ w_2 \\ \vdots \\ \vdots \\ w_{T+L} \\ w_{T+L+1} \end{bmatrix}}_{\boldsymbol{w}}. \tag{3.16}$$

This structure can be adapted to a general MIMO system as will be discussed in Section 4.3.

In order to apply SD based on the complex model given in (3.14), we transform

$\boldsymbol{s}$, $\boldsymbol{y}$, $\boldsymbol{w}$ and $\boldsymbol{H}$ to their real equivalent forms as

$$\begin{aligned}
\mathbf{s} &= \left[\mathrm{Re}(\boldsymbol{s})^T \ \mathrm{Im}(\boldsymbol{s})^T\right]^T, \\
\mathbf{y} &= \left[\mathrm{Re}(\boldsymbol{y})^T \ \mathrm{Im}(\boldsymbol{y})^T\right]^T, \\
\mathbf{w} &= \left[\mathrm{Re}(\boldsymbol{w})^T \ \mathrm{Im}(\boldsymbol{w})^T\right]^T, \\
\mathbf{H} &= \begin{bmatrix} \mathrm{Re}(\tilde{\boldsymbol{H}}) & \mathrm{Im}(\tilde{\boldsymbol{H}}) \\ -\mathrm{Im}(\tilde{\boldsymbol{H}}) & \mathrm{Re}(\tilde{\boldsymbol{H}}) \end{bmatrix},
\end{aligned}$$

respectively, where, in general, we assume $\mathbf{s} \in \mathbb{R}^m$, $\mathbf{y}, \mathbf{w} \in \mathbb{R}^n$ and $\mathbf{H} \in \mathbb{R}^{n \times m}$. $\mathrm{Re}(\cdot)$ and $\mathrm{Im}(\cdot)$ denote the real and imaginary part of a complex vector/matrix, respectively.

The model (3.14) now can be written in its real-equivalent form as

$$\mathbf{y} = \mathbf{H}\mathbf{s} + \mathbf{w}. \tag{3.17}$$

Because of assumption of elements of $\boldsymbol{w}$ in (3.14), it follows that $\mathbf{w}$ in (3.17) comprises of i.i.d. real Gaussian random variables with zero mean and a common variance. The symbol vector $\mathbf{s}$ is uniformly distributed over a discrete and finite set $\mathcal{C} \subset \mathbb{R}^m$. We assume that the complex symbols s_i of $\boldsymbol{s}$ belong to a QAM constellation, i.e., $\mathcal{C} = \mathcal{X}^m$, where $\mathcal{X}$ is a PAM signal set of size Q. More explicitely,

$$\mathcal{X} = \{u = 2q - Q + 1 : q \in \mathbb{Z}_Q\}. \tag{3.18}$$

Under these conditions and assuming that $\mathbf{H}$ is perfectly known at the receivers, the optimal detector $g : \mathbf{y} \longmapsto \hat{\mathbf{s}} \in \mathcal{C}$ that minimizes the average symbol error probability

$$Pr(e) \triangleq Pr(\hat{\mathbf{s}} \neq \mathbf{s})$$

is the ML detector given by

$$\hat{\mathbf{s}} = \arg\min_{\mathbf{s}\in\mathcal{C}} \|\mathbf{y} - \mathbf{H}\mathbf{s}\|^2. \tag{3.19}$$

By applying a suitable translation and scaling of the received signal vector, (3.19) takes on the form

$$\hat{\mathbf{s}} = \arg\min_{\mathbf{s}\in\mathbb{Z}_Q^m} \|\mathbf{y} - \mathbf{H}\mathbf{s}\|^2 \tag{3.20}$$

and this corresponds to the problem of (3.13) in section 3.3.

One scenario we can encounter in practice is when $\boldsymbol{w}$ of (3.14) does not consist of independent Gaussian random variables but correlated Gaussian random variables (colored noise), i.e., $\boldsymbol{w} \sim \mathcal{CN}(\mathbf{0}, \boldsymbol{\Sigma})$ where $\boldsymbol{\Sigma}$ is the covariance matrix and $\boldsymbol{\Sigma}$ is no longer of diagonal form. In this case, in order to apply the Sphere Decoder developed for the white noise case, we employ Cholesky decomposition [24] and write $\boldsymbol{\Sigma} = \boldsymbol{G}\boldsymbol{G}^{\mathcal{H}}$ where $\boldsymbol{G}$ is a lower triangular matrix. We multiply both sides of (3.14) with $\boldsymbol{G}^{-1}$ to obtain

$$\boldsymbol{G}^{-1}\boldsymbol{y} = \boldsymbol{G}^{-1}\tilde{\boldsymbol{H}}\boldsymbol{s} + \boldsymbol{G}^{-1}\boldsymbol{w} \tag{3.21}$$

or equivalently

$$\boldsymbol{y}^{'} = \tilde{\boldsymbol{H}}^{'}\boldsymbol{s} + \boldsymbol{w}^{'}. \tag{3.22}$$

where $\boldsymbol{y}^{'}$, $\tilde{\boldsymbol{H}}^{'}$ and $\boldsymbol{w}^{'}$ are, respectively, $\boldsymbol{y}$, $\tilde{\boldsymbol{H}}$ and $\boldsymbol{w}$ premultiplied with $\boldsymbol{G}^{-1}$.

It is easy to see that the covariance matrix of $\boldsymbol{w}^{'}$ satisfies

$$\begin{aligned} E\left\{\boldsymbol{w}^{'}(\boldsymbol{w}^{'})^{\mathcal{H}}\right\} &= E\left\{\boldsymbol{G}^{-1}\mathbf{w}\mathbf{w}^{\mathcal{H}}(\boldsymbol{G}^{-1})^{\mathcal{H}}\right\} \\ &= \boldsymbol{G}^{-1}\boldsymbol{\Sigma}(\boldsymbol{G}^{-1})^{\mathcal{H}} = \boldsymbol{G}^{-1}\boldsymbol{G}\boldsymbol{G}^{\mathcal{H}}(\boldsymbol{G}^{-1})^{\mathcal{H}} = \boldsymbol{I}. \end{aligned} \tag{3.23}$$

We then transform (3.22) to its real-equivalent form and perform the needed transformation and scaling operations on $\boldsymbol{y}^{'}$, to reduce the problem to that of (3.20).

3.5 Summary

In this chapter, we investigated the integer least-squares problem for infinite and finite integer lattice. By inspecting the Pohst and Schnorr-Euchner enumerations to solve the problem for infinite integer lattices, the problem for finite integer lattice is deduced. It turns out that the ML detection in many communication problems can lead to the least-squares problems for finite integer lattice. The algorithm to find the ML estimations based on Sphere Decoding is discussed for the case of white noise and colored noise.

CHAPTER 4

CHANNEL ESTIMATION AND DETECTION FOR MIMO SYSTEMS

4.1 Decouple Maximum Likelihood (DEML)

We consider a general estimation problem which is expressed in (4.1) below

$$\boldsymbol{Y} = \boldsymbol{H}\boldsymbol{S} \ + \ \boldsymbol{W} \tag{4.1}$$

where $\boldsymbol{Y} = [\boldsymbol{y}(0)\ \boldsymbol{y}(1)\ \cdots\ \boldsymbol{y}(n)] \in \mathbb{C}^{m\times n}$, $\boldsymbol{H} \in \mathbb{C}^{m\times l}$, $\boldsymbol{S} \in \mathcal{C}^{l\times n}$ and $\boldsymbol{W} = [\boldsymbol{w}(0)\ \boldsymbol{w}(1)\ \cdots \boldsymbol{w}(n)] \in \mathbb{C}^{m\times n}$. Each column of $\boldsymbol{W}$, $\boldsymbol{w}(i),\ i = 1, 2, \cdots, n$ is a realization of a random complex Gaussian vector of zero mean and covariance matrix of $E\left\{\boldsymbol{w}(i)\boldsymbol{w}(i)^{\mathcal{H}}\right\} = \boldsymbol{\Sigma}$. The problem we would like to address is when $\boldsymbol{Y}$, $\boldsymbol{S}$ are known, how to determine the $\boldsymbol{H}$ and the covariance matrix $\boldsymbol{\Sigma}$.

For a given $\boldsymbol{S}$, the probability density function (pdf) of the i^{th} column of $\boldsymbol{Y}$, $\boldsymbol{y}(i)$, is

$$f_{\boldsymbol{y}(i)|\boldsymbol{H},\boldsymbol{\Sigma},\boldsymbol{S}}\big(\boldsymbol{y}(i)|\boldsymbol{H},\boldsymbol{\Sigma},\boldsymbol{S}\big) = \frac{1}{|\pi\boldsymbol{\Sigma}|}\exp\Big\{-\big(\boldsymbol{y}(i) - E\left\{\boldsymbol{y}(i)\right\}\big)^{\mathcal{H}}\boldsymbol{\Sigma}^{-1}\big(\boldsymbol{y}(i) - E\left\{\boldsymbol{y}(i)\right\}\big)\Big\} \tag{4.2}$$

Therefore,

$$\begin{aligned} f_{\boldsymbol{Y}|\boldsymbol{H},\boldsymbol{\Sigma},\boldsymbol{S}}\big(\boldsymbol{Y}|\boldsymbol{H},\boldsymbol{\Sigma},\boldsymbol{S}\big) &= \prod_{i=1}^{n} f_{\boldsymbol{y}(i)|\boldsymbol{H},\boldsymbol{\Sigma},\boldsymbol{S}}\big(\boldsymbol{y}(i)|\boldsymbol{H},\boldsymbol{\Sigma},\boldsymbol{S}\big) \\ &= \frac{1}{|\pi\boldsymbol{\Sigma}|^{n}}\exp\left\{-\mathrm{tr}\left[(\boldsymbol{Y} - \boldsymbol{H}\boldsymbol{S})^{\mathcal{H}}\boldsymbol{\Sigma}^{-1}(\boldsymbol{Y} - \boldsymbol{H}\boldsymbol{S})\right]\right\}. \end{aligned} \tag{4.3}$$

The log-likelihood function of $\boldsymbol{Y}$ given $\boldsymbol{S}$ is proportional to (within an additive constant) [18]

$$F_1 = -\log|\boldsymbol{\Sigma}| - \frac{1}{n}\mathrm{tr}\big[\boldsymbol{\Sigma}^{-1}(\boldsymbol{Y} - \boldsymbol{H}\boldsymbol{S})(\boldsymbol{Y} - \boldsymbol{H}\boldsymbol{S})^{\mathcal{H}}\big]. \tag{4.4}$$

In order to maximize F_1 with respect to (w.r.t) $\boldsymbol{\Sigma}$, we take the derivative of F_1 w.r.t $\boldsymbol{\Sigma}$ and equate it to 0 as follows:

$$\begin{aligned}\frac{dF_1}{d\boldsymbol{\Sigma}} &= -n\boldsymbol{\Sigma}^{-1} - \boldsymbol{\Sigma}^{-1}(\boldsymbol{Y}-\boldsymbol{H}\boldsymbol{S})(\boldsymbol{Y}-\boldsymbol{H}\boldsymbol{S})^{\mathcal{H}}\boldsymbol{\Sigma}^{-1} = 0 \\ \Longleftrightarrow \boldsymbol{\Sigma} &= \frac{1}{n}(\boldsymbol{Y}-\boldsymbol{H}\boldsymbol{S})(\boldsymbol{Y}-\boldsymbol{H}\boldsymbol{S})^{\mathcal{H}} \equiv \hat{\boldsymbol{\Sigma}} \end{aligned} \tag{4.5}$$

Substituting (4.5) into (4.4), we have

$$\begin{aligned} F_1|_{\boldsymbol{\Sigma}=\hat{\boldsymbol{\Sigma}}} &= -n\log|\hat{\boldsymbol{\Sigma}}| - \mathrm{tr}[(\boldsymbol{Y}-\boldsymbol{H}\boldsymbol{S})^{\mathcal{H}}\hat{\boldsymbol{\Sigma}}^{-1}(\boldsymbol{Y}-\boldsymbol{H}\boldsymbol{S})] \\ &= -n\log|\hat{\boldsymbol{\Sigma}}| - \mathrm{tr}[\hat{\boldsymbol{\Sigma}}^{-1}(\boldsymbol{Y}-\boldsymbol{H}\boldsymbol{S})(\boldsymbol{Y}-\boldsymbol{H}\boldsymbol{S})^{\mathcal{H}}] \\ &= -n\log|\hat{\boldsymbol{\Sigma}}| - \mathrm{tr}[n\hat{\boldsymbol{\Sigma}}^{-1}\hat{\boldsymbol{\Sigma}}] \\ &= -n\log|\hat{\boldsymbol{\Sigma}}| - nm. \end{aligned} \tag{4.6}$$

Therefore, we can obtain the estimate $\hat{\boldsymbol{H}}$ (in order to maximize $F_1|_{\boldsymbol{\Sigma}=\hat{\boldsymbol{\Sigma}}}$) by minimizing $\log|\hat{\boldsymbol{\Sigma}}|$. Let

$$F_2 = \log|\hat{\boldsymbol{\Sigma}}| = \left|\frac{1}{n}(\boldsymbol{Y}-\boldsymbol{H}\boldsymbol{S})(\boldsymbol{Y}-\boldsymbol{H}\boldsymbol{S})^{\mathcal{H}}\right| \tag{4.7}$$

Let $\hat{\boldsymbol{R}}_{\boldsymbol{YY}} = \frac{1}{n}\boldsymbol{Y}\boldsymbol{Y}^{\mathcal{H}}$, $\hat{\boldsymbol{R}}_{\boldsymbol{SS}} = \frac{1}{n}\boldsymbol{S}\boldsymbol{S}^{\mathcal{H}}$ and $\hat{\boldsymbol{R}}_{\boldsymbol{SY}} = \frac{1}{n}\boldsymbol{S}\boldsymbol{Y}^{\mathcal{H}}$ and define

$$\begin{aligned} \boldsymbol{C} &= \frac{1}{n}(\boldsymbol{Y}-\boldsymbol{H}\boldsymbol{S})(\boldsymbol{Y}-\boldsymbol{H}\boldsymbol{S})^{\mathcal{H}} \\ &= \left[\boldsymbol{H} - \hat{\boldsymbol{R}}_{\boldsymbol{SY}}^{\mathcal{H}}\hat{\boldsymbol{R}}_{\boldsymbol{SS}}^{-1}\right]\hat{\boldsymbol{R}}_{\boldsymbol{SS}}\left[\boldsymbol{H} - \hat{\boldsymbol{R}}_{\boldsymbol{SY}}^{\mathcal{H}}\hat{\boldsymbol{R}}_{\boldsymbol{SS}}^{-1}\right]^{\mathcal{H}} \\ &\quad + \hat{\boldsymbol{R}}_{\boldsymbol{YY}} - \hat{\boldsymbol{R}}_{\boldsymbol{SY}}^{\mathcal{H}}\hat{\boldsymbol{R}}_{\boldsymbol{SS}}^{-1}\hat{\boldsymbol{R}}_{\boldsymbol{SY}} \end{aligned} \tag{4.8}$$

Since $\hat{\boldsymbol{R}}_{\boldsymbol{SS}}$ is positive definite (hence the first term in (4.8) is nonnegative) and the second and third term do not depend on $\boldsymbol{H}$, it follows that

$$\boldsymbol{C} \geq \boldsymbol{C}|_{\boldsymbol{H}=\hat{\boldsymbol{H}}} \tag{4.9}$$

where

$$\hat{\boldsymbol{H}} = \hat{\boldsymbol{R}}_{\boldsymbol{SY}}^{\mathcal{H}}\hat{\boldsymbol{R}}_{\boldsymbol{SS}}^{-1} \tag{4.10}$$

The inequality expression in (4.9) means that the difference matrix $\boldsymbol{C} - \boldsymbol{C}|_{\boldsymbol{H}=\hat{\boldsymbol{H}}}$ is nonnegative definite. Since the whole sample covariance matrix $\boldsymbol{C}$ is minimized, the estimate $\hat{\boldsymbol{H}}$ of $\boldsymbol{H}$ will minimize any nondecreasing function[1] of $\boldsymbol{C}$ including the determinant of $\boldsymbol{C}$ which is F_2 in (4.7). Thus, the ML estimate of $\boldsymbol{H}$ is gven by (4.10).

Substituting (4.10) back to (4.5), we obtain the ML estimate of $\boldsymbol{\Sigma}$

$$\hat{\boldsymbol{\Sigma}} = \hat{\boldsymbol{R}}_{\boldsymbol{YY}} - \hat{\boldsymbol{R}}_{\boldsymbol{SY}}^{\mathcal{H}} \hat{\boldsymbol{R}}_{\boldsymbol{SS}}^{-1} \hat{\boldsymbol{R}}_{\boldsymbol{SY}}. \tag{4.11}$$

In this way, we decouple the multi-dimensional problem of exact maximum likelihood estimator in (4.4) in to a set of one dimensional problems as given by (4.10) and (4.11). A decoupled maximum likelihood (DEML) estimator is established.

4.2 Channel estimation and Detection for quasi-static flat fading channels

4.2.1 System model

We consider a MIMO system having N_i transmitters and N_0 receivers whose discrete-time model is addressed in Chapter 2. There are a total of $N_i N_0$ links in our system of which the channel impulse response of the link from i^{th} transmitter to j^{th} receivers is $h^{(i,j)}(k) = h_{i,j}\delta(k),\ i = 1, 2, \cdots, N_i,\ j = 1, 2, \cdots, N_0$. $h_{i,j}$ is modeled as a complex Gaussian random variable. Furthermore, $h_{i,j}$ is assumed to be unchanged during a block of N symbols and changed randomly from block to block.

[1] A function $h(\boldsymbol{C})$ is a nondecreasing function of a positive definite $\boldsymbol{C}$ if for any nonnegative definite $\Delta\boldsymbol{C}$, $h(\boldsymbol{C} + \Delta\boldsymbol{C}) \geq h(\boldsymbol{C})$, and the equality holds only for $\Delta\boldsymbol{C} = \boldsymbol{0}$[25]

With these assumptions, at any discrete time instance k, the received signals at the N_0 receivers can be written as a linear combination of the transmitted signals from N_i transmitters using matrix notation as

$$\begin{bmatrix} y^{(1)}(k) \\ y^{(2)}(k) \\ \vdots \\ y^{(N_0)}(k) \end{bmatrix} = \begin{bmatrix} h_{1,1} \cdots\cdots h_{N_i,1} \\ h_{1,1} \cdots\cdots h_{N_i,1} \\ \vdots \quad \vdots \ddots \quad \vdots \\ h_{1,N_0} \cdots\cdots h_{N_i,N_0} \end{bmatrix} \begin{bmatrix} s^{(1)}(k) \\ s^{(2)}(k) \\ \vdots \\ s^{(N_i)}(k) \end{bmatrix} + \begin{bmatrix} w^{(1)}(k) \\ w^{(2)}(k) \\ \vdots \\ w^{(N_0)}(k) \end{bmatrix}$$

or

$$\boldsymbol{y}(k) = \boldsymbol{H}\boldsymbol{s}(k) + \boldsymbol{w}(k) \tag{4.12}$$

where $y^{(j)}(k)$, $s^{(i)}(k)$, $w^{(j)}(k)$ is the received signal from the j^{th} receiver, transmitted signal from i^{th} transmitter, additive noise at the j^{th} receiver at time k, respectively. $h_{i,j}$ is the channel impulse response from i^{th} transmitter to j^{th} receiver, $i = 1, 2, \cdots, N_i$, $j = 1, 2, \cdots, N_0$. $\boldsymbol{y}(k) \in \mathbb{C}^{N_0 \times 1}$, $\boldsymbol{s}(k) \in \mathcal{C}^{N_i \times 1}$, $\boldsymbol{w}(k) \in \mathbb{C}^{N_0 \times 1}$ and $\boldsymbol{H} \in \mathbb{C}^{N_0 \times N_i}$. The noise at the receivers are assumed to be temporally white but dependent among the receivers, i.e., $E\left\{\boldsymbol{w}(t_1)\boldsymbol{w}(t_2)^{\mathcal{H}}\right\} = \boldsymbol{\Sigma} \times \delta(t_1 - t_2)$.

If we assume that the LOS path does not exist in each link of our system, then $h_{i,j}$ is a complex Gaussian random variable with zero mean and variance of σ^2. Thus, the total transmit SNR over all antennas is

$$\mathrm{SNR}_{total} = N_i \frac{P_s \sigma^2}{\sigma_w^2} \tag{4.13}$$

where σ_w^2 is the variance of noise at each receiver and $P_s/2$ is the average power of constellation in use.

The per-antenna SNR is

$$\mathrm{SNR} = \frac{\mathrm{SNR}_{total}}{N_i} = \frac{P_s \sigma^2}{\sigma_w^2} \tag{4.14}$$

If, in each link of our system, there is a LOS path, then Ricean fading distribution is used to model the statistics of $h_{i,j}$ as

$$h_{i,j} = A + v_{i,j} \tag{4.15}$$

where A denotes the peak amplitude of the LOS signal and $v_{i,j}$ is a complex Gaussian random variable with zero mean and variance of σ^2. The relationship between A and σ^2 is expressed by Rician factor K given by $K = A^2/(2\sigma^2)$. In this case, the the total transmit SNR over all antennas is

$$\text{SNR}_{total} = N_i \frac{P_s(A^2/2 + \sigma^2)}{\sigma_w^2} \tag{4.16}$$

The per-antenna SNR is

$$\text{SNR} = \frac{\text{SNR}_{total}}{N_i} = \frac{P_s(A^2/2 + \sigma^2)}{\sigma_w^2} \tag{4.17}$$

In all our simulations, the BER performance is sketched as a function of per-antenna SNR.

During the N symbol periods over which the channels remain unchanged, the transmitted signals from a specific transmit antenna has the structure depicted in Figure 4.1. In which, the first M symbols of each block of N symbols are used for estimation of channel information, more explicitly, to estimate $\boldsymbol{H}$ and $\boldsymbol{\Sigma}$.

4.2.2 Channel estimation

During the first M pilot symbols of a block of N symbols, we group M received signal vectors at the receivers to form a matrix of $\boldsymbol{Y} = [\boldsymbol{y}(0)\ \boldsymbol{y}(1)\ \cdots\ \boldsymbol{y}(M-1)] \in \mathbb{C}^{N_0 \times M}$, then $\boldsymbol{Y}$ can be written as

$$\boldsymbol{Y} = \boldsymbol{H}\boldsymbol{S} + \boldsymbol{W} \tag{4.18}$$

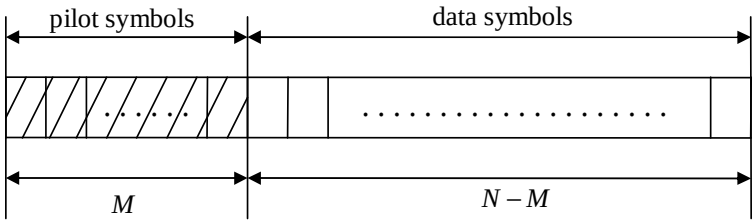

Figure 4.1: Symbols structure for flat fading channels.

where $\boldsymbol{S} = [\boldsymbol{s}(0)\ \boldsymbol{s}(1)\ \cdots\ \boldsymbol{s}(M-1)]$ and $\boldsymbol{W} = [\boldsymbol{w}(0)\ \boldsymbol{w}(1)\ \cdots\ \boldsymbol{w}(M-1)] \in \mathbb{C}^{N_0 \times M}$.

From the DEML estimator of Section 4.1, the estimation of $\boldsymbol{H}$ and $\boldsymbol{\Sigma}$ are

$$\hat{\boldsymbol{H}} = \hat{\boldsymbol{R}}_{\boldsymbol{SY}}^{\mathcal{H}} \hat{\boldsymbol{R}}_{\boldsymbol{SS}}^{-1} \tag{4.19}$$

$$\hat{\boldsymbol{\Sigma}} = \hat{\boldsymbol{R}}_{\boldsymbol{YY}} - \hat{\boldsymbol{R}}_{\boldsymbol{SY}}^{\mathcal{H}} \hat{\boldsymbol{R}}_{\boldsymbol{SS}}^{-1} \hat{\boldsymbol{R}}_{\boldsymbol{SY}} \tag{4.20}$$

where $\hat{\boldsymbol{R}}_{\boldsymbol{YY}} = \frac{1}{M}\boldsymbol{Y}\boldsymbol{Y}^{\mathcal{H}}$, $\hat{\boldsymbol{R}}_{\boldsymbol{SY}} = \frac{1}{M}\boldsymbol{S}\boldsymbol{Y}^{\mathcal{H}}$, $\hat{\boldsymbol{R}}_{\boldsymbol{SS}} = \frac{1}{M}\boldsymbol{S}\boldsymbol{S}^{\mathcal{H}}$.

4.2.3 Symbol Detection

In this section, we describe how to use the estimates from the section 4.2.2 to decode the transmitted signals. Here, we assume $\boldsymbol{H}$ and $\boldsymbol{\Sigma}$ have been determined by our DEML algorithm.

In every block of transmitted signals from the transmitters, the last $N - M$ symbols are data symbols. At any time $k = M+1, M+2, \cdots, N$ the output-input relationship is written as

$$\boldsymbol{y}(k) = \boldsymbol{H}\boldsymbol{s}(k) + \boldsymbol{w}(k) \tag{4.21}$$

In order to apply SD in the detection process, (4.21) is post-multiplied with

$\boldsymbol{G}^{-1}$ where $\boldsymbol{G}\boldsymbol{G}^{\mathcal{H}} = \boldsymbol{\Sigma}$ to form

$$\begin{aligned} \boldsymbol{G}^{-1}\boldsymbol{y}(k) &= \boldsymbol{G}^{-1}\boldsymbol{H}\boldsymbol{s}(k) + \boldsymbol{G}^{-1}\boldsymbol{w}(k) \\ \boldsymbol{y}^{'}(k) &= \boldsymbol{H}^{'}\boldsymbol{s}(k) + \boldsymbol{w}^{'}(k) \end{aligned} \tag{4.22}$$

and SD is applied in (4.22) (after transforming to its real-equivalent form) to find the ML estimation of transmitted symbol vector $\boldsymbol{s}(k)$ at time k.

4.3 Channel estimation and detection for quasi-static frequency selective fading channels

4.3.1 System model

We consider the discrete-time block transmission equivalent model of a baseband MIMO communication systems having N_i transmitters and N_0 receivers in Chapter 2. There are total of N_iN_0 links in this MIMO systems. We assume that the link between each transmitter-receiver pair is modeled as a finite impulse response (FIR) dispersive channel which has no greater than $(L+1)$ symbol-spaced taps in the channel response. The sampled channel response between i^{th} transmitter and j^{th} receiver is denoted by $\boldsymbol{h}^{(i,j)} = [h_{i,j}(0)\ h_{i,j}(1)\ \cdots\ h_{i,j}(L)]^T \in \mathbb{C}^{(L+1)\times 1}$ where $h_{i,j}(l), 1 \leq i \leq N_i, 1 \leq j \leq N_0, 0 \leq l \leq L$ are independent identical complex Gaussian random variables. We denote $\boldsymbol{h}^{(i)}(l) = [h_{i,1}(l)\ h_{i,2}(l)\ \cdots\ h_{i,N_0}(l)]^T \in \mathbb{C}^{N_0\times 1}, l = 0, 1, \cdots, L$ as the channel from i^{th} transmitter to all N_0 receivers at l^{th} tap.

In our system, we adopt a block transmission structure with zero-padding to eliminate interblock interference, hence alleviating the performance degration due to IBI from the previous block onto the current block as discussed in Chapter 2. At each transmitter, information-bearing symbols are divided into $N-$ long

blocks, with the insertion of $T \geq L$ zeros symbols at the tail of each block to form a frame having the length of $D = N+T$ symbol periods. We denote the n^{th} block of the i^{th} transmitter as $\boldsymbol{s}_n^{(i)} = \left[s_n^{(i)}(nN)\ s_n^{(i)}(nN+1)\ \cdots\ s_n^{(i)}(nN+N-1)\right]^T$. After zero padding , each $N-$ long information-bearing block $\boldsymbol{s}_n^{(i)}$ creates a transmit frame $\bar{\boldsymbol{s}}_n^{(i)} = [\bar{s}_n^{(i)}(nD)\ \bar{s}_n^{(i)}(nD+1)\ \cdots\ \bar{s}_n^{(i)}(nD+D-1)]^T$ of frame size D, where the first N entries convey messages $\bar{s}_n^{(i)}(nD+k) = s_n^{(i)}(nN+k)$ for $k = 0, 1, 2, \cdots, N-1$, followed by T trialling zeros $\bar{s}_n^{(i)}(nD+k) = 0$ for $k = N, N+1, N+2, \cdots, D-1$, for any frame index n and any transmitter $i \in [1, N_i]$.

At the receiving premise, during the process of receiving the n^{th} data frames from N_i transmitters, we collect N_0 samples from the outputs of N_0 receivers at time $(nD+k)$ to form $\boldsymbol{y}_n(nD+k) = \left[y_n^{(1)}(nD+k)\ y_n^{(2)}(nD+k)\ \cdots\ y_n^{(N_0)}(nD+k)\right]^T \in \mathbb{C}^{N_0 \times 1}$ where $y_n^{(j)}(nD+k)$ denotes the sample from j^{th} receiver at time $(nD+k)$, $k = 0, 1, \cdots, D-1$. This sample is contaminated by $w_n^{(j)}(nD+k)$ which is an complex Gaussian random variable. The $y_n^{(j)}(nD+k)$ can be determined by

$$\begin{aligned} y_n^{(j)}(nD+k) &= \sum_{i=1}^{N_i} \sum_{m=0}^{L} h_{i,j}(m) \bar{s}_n^{(i)}(nD+k-m) + w^{(j)}(nD+k) \\ &= \sum_{m=0}^{L} h_{1,j}(m) \bar{s}_n^{(1)}(nD+k-m) \ + \ \cdots \\ &\quad + \sum_{m=0}^{L} h_{N_i,j}(m) \bar{s}_n^{(N_i)}(nD+k-m) + w_n^{(j)}(nD+k). \quad (4.23) \end{aligned}$$

Therefore, $\boldsymbol{y}_n(nD+k)$ can be evaluated as

$$\begin{aligned} \boldsymbol{y}_n(nD+k) &= \sum_{m=0}^{L} \boldsymbol{h}^{(1)}(m) \bar{s}_n^{(1)}(nD+k-m) + \cdots \\ &\quad + \sum_{m=0}^{L} \boldsymbol{h}^{(N_i)}(m) \bar{s}_n^{(N_i)}(nD+k-m) + \boldsymbol{w}_n(nD+k). \quad (4.24) \end{aligned}$$

We model $\boldsymbol{w}_n(nD+k)$ a complex Gaussian vector with zero-mean and

$E\{\boldsymbol{w}_n(nD+k_1)\boldsymbol{w}_n^{\mathcal{H}}(nD+k_2)\} = \boldsymbol{\Sigma} \times \delta(t_1 - t_2)$, that is, our noise is temporally white, $\boldsymbol{w}(t) \sim \mathcal{CN}(0, \boldsymbol{\Sigma})$ where $\boldsymbol{\Sigma}$ is the $N_0 \times N_0$ covariance matrix of $\boldsymbol{w}(t)$ to be determined.

Thus, equation (4.24) can be written as

$$\boldsymbol{y}_n(nD+k) = \begin{bmatrix}\boldsymbol{h}^{(1)}(0) & \cdots & \boldsymbol{h}^{(1)}(L)\end{bmatrix} \begin{bmatrix} \bar{s}_n^{(1)}(nD+k) \\ \bar{s}_n^{(1)}(nD+k-1) \\ \vdots \\ \bar{s}_n^{(1)}(nD+k-L) \end{bmatrix} + \cdots$$

$$+ \begin{bmatrix}\boldsymbol{h}^{(N_i)}(0) & \cdots & \boldsymbol{h}^{(N_i)}(L)\end{bmatrix} \begin{bmatrix} \bar{s}_n^{(Ni)}(nD+k) \\ \bar{s}_n^{(N_i)}(nD+k-1) \\ \vdots \\ \bar{s}_n^{(N_i)}(nD+k-L) \end{bmatrix} + \boldsymbol{w}_n(nD+k) \quad (4.25)$$

If we define $\bar{\boldsymbol{s}}_n^{(i)}(m) = \begin{bmatrix}\bar{s}_n^{(i)}(m) & \cdots & \bar{s}_n^{(i)}(m-L)\end{bmatrix}^T, i = 1, 2, \cdots, N_i$ and $\boldsymbol{H}^{(i)} = \begin{bmatrix}\boldsymbol{h}^{(i)}(0) & \cdots & \boldsymbol{h}^{(i)}(L)\end{bmatrix}$ then (4.25) can be written as

$$\boldsymbol{y}_n(nD+k) = \begin{bmatrix}\boldsymbol{H}^{(1)} & \boldsymbol{H}^{(2)} \cdots & \boldsymbol{H}^{(N_i)}\end{bmatrix} \begin{bmatrix} \bar{\boldsymbol{s}}_n^{(1)}(nD+k) \\ \bar{\boldsymbol{s}}_n^{(2)}(nD+k) \\ \vdots \\ \bar{\boldsymbol{s}}_n^{(N_i)}(nD+k) \end{bmatrix} + \boldsymbol{w}_n(nD+k) \quad (4.26)$$

or equivalently

$$\boldsymbol{y}_n(nD+k) = \boldsymbol{H}\bar{\boldsymbol{s}}(nD+k) + \boldsymbol{w}_n(nD+k) \quad (4.27)$$

where $\boldsymbol{H} = \begin{bmatrix}\boldsymbol{H}^{(1)} & \boldsymbol{H}^{(2)} \cdots & \boldsymbol{H}^{(N_i)}\end{bmatrix} \in \mathbb{C}^{N_0 \times N_i(L+1)}$ and $\bar{\boldsymbol{s}}_n(nD+k) = \begin{bmatrix}\bar{\boldsymbol{s}}_n^{(1)}(nD+k)^T & \bar{\boldsymbol{s}}_n^{(2)}(nD+k)^T & \cdots & \bar{\boldsymbol{s}}_n^{(N_i)}(nD+k)^T\end{bmatrix}^T$.

Because of zero padding, IBI is avoided and we may simply omit the adjacent frames and consider only one frame. Hereon, we may drop the frame index n

to simplify our notation.

The structure of a frame from a transmitter is illustrated in Figure 4.2.

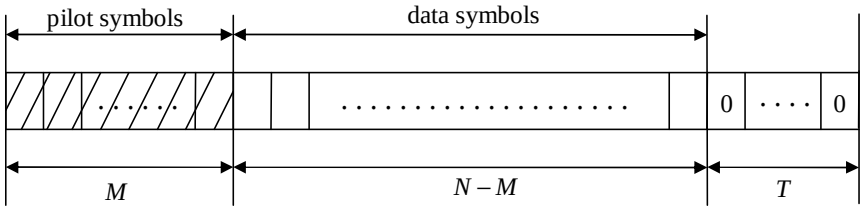

Figure 4.2: Symbols structure for frequency selective fading channels.

If there is no LOS path in our system, then the channel coefficient $h_{i,j}(l)$, $i = 1, 2, \cdots, N_i; j = 1, 2, \cdots, N_0; l = 0, 1, \cdots, L$, can be modeled as a complex Gaussian random variable with zero-mean and variance of σ_l^2. Thus the per-antenna SNR is

$$\text{SNR} = \frac{P_s \sum_{l=0}^{L} \sigma_l^2}{\sigma_w^2} \tag{4.28}$$

If there is a LOS path in each link in our system, then all the coefficients $h_{i,j}(l)$, $i = 1, 2, \cdots, N_i; j = 1, 2, \cdots, N_0; l = 1, \cdots, L$ are modeled as complex Gaussian random variables with zero-mean and variance of σ_l^2, with the coefficient $h_{i,j}(0)$ modeled as

$$h_{i,j}(0) = A + v_{i,j}(0) \tag{4.29}$$

where A denotes the peak amplitude of LOS signal and $v_{i,j}(0)$ is a complex Gaussian random variable with zero-mean and variance of σ_0^2. Here, we modify the Rician factor as

$$K = \frac{A^2/2}{\sum_{l=0}^{L} \sigma_l^2}. \tag{4.30}$$

Therefore, the per-antenna SNR is

$$\text{SNR} = \frac{P_s(A^2/2 + \sum_{l=0}^{L} \sigma_l^2)}{\sigma_w^2} \tag{4.31}$$

where σ_w^2 is the variance of noise at each receiver.

4.3.2 Channel estimation

The first M symbols of each frame from each transmitter are used for the purpose of obtaining the information of channel that is needed in detection stage.

During the training period, we group M vectors of received signals from all N_0 receivers to form $\boldsymbol{Y} = [\boldsymbol{y}(0)\ \boldsymbol{y}(1)\ \cdots\ \boldsymbol{y}(M-1)] \in \mathbb{C}^{N_0 \times M}$. This matrix can be written as

$$\boldsymbol{Y} = \boldsymbol{H}\bar{\boldsymbol{S}}\ +\ \boldsymbol{W} \tag{4.32}$$

where $\bar{\boldsymbol{S}} = [\bar{\boldsymbol{s}}(0)\ \bar{\boldsymbol{s}}(1)\ \cdots\ \bar{\boldsymbol{s}}(M-1)]$ and $\boldsymbol{N} = [\boldsymbol{w}(0)\ \boldsymbol{w}(1)\ \cdots\ \boldsymbol{w}(M-1)] \in \mathbb{C}^{N_0 \times M}$.

Let $\hat{\boldsymbol{R}}_{\boldsymbol{YY}} = \frac{1}{M}\boldsymbol{Y}\boldsymbol{Y}^{\mathcal{H}}$, $\hat{\boldsymbol{R}}_{\bar{\boldsymbol{S}}\bar{\boldsymbol{S}}} = \frac{1}{M}\bar{\boldsymbol{S}}\boldsymbol{S}^{\mathcal{H}}$ and $\hat{\boldsymbol{R}}_{\bar{\boldsymbol{S}}\boldsymbol{Y}} = \frac{1}{M}\bar{\boldsymbol{S}}\boldsymbol{Y}^{\mathcal{H}}$. From the DEML estimator, we have the estimated value of $\boldsymbol{H}$ and $\boldsymbol{\Sigma}$ as

$$\hat{\boldsymbol{H}} = \hat{\boldsymbol{R}}^{\mathcal{H}}_{\bar{\boldsymbol{S}}\boldsymbol{Y}}\hat{\boldsymbol{R}}^{-1}_{\bar{\boldsymbol{S}}\bar{\boldsymbol{S}}} \tag{4.33}$$

and

$$\hat{\boldsymbol{\Sigma}} = \hat{\boldsymbol{R}}_{\boldsymbol{YY}} - \hat{\boldsymbol{R}}^{\mathcal{H}}_{\bar{\boldsymbol{S}}\boldsymbol{Y}}\hat{\boldsymbol{R}}^{-1}_{\bar{\boldsymbol{S}}\bar{\boldsymbol{S}}}\hat{\boldsymbol{R}}_{\bar{\boldsymbol{S}}\boldsymbol{Y}} \tag{4.34}$$

4.3.3 Symbol Detection

In this section, we describe how to use the estimates obtained from DEML estimator for symbol detection. From now on, in every equation, we assume $\boldsymbol{H}$ and $\boldsymbol{\Sigma}$ have been determined by our DEML algorithm.

The data received after training symbols are $\{\boldsymbol{y}(k)\}_{k=M}^{D-1}$ which are determined as

$$\boldsymbol{y}(k) = \boldsymbol{H}\bar{\boldsymbol{s}}(k)\ +\ \boldsymbol{w}(k) \tag{4.35}$$

From these received data, a ML estimation of the information-bearing symbols can be easily established. However, it will incur exponential complexity with respect to frame length and hence has little practical usage.

We will apply the Sphere Decoder into symbol detection by dividing the $\{\boldsymbol{y}(k)\}_{k=M}^{D-1}$ into subframe of length P. The value of P is the tradeoff between the system's performance and the complexity of detection stage. We denote a subframe as $\boldsymbol{y}_P(j) = \left[\boldsymbol{y}^T(jP+M)\ \boldsymbol{y}^T(jP+M+1)\ \cdots\ \boldsymbol{y}^T(jP+P+M-1)\right]^T \in \mathbb{C}^{PN_0\times 1}$ and we define

$$\mathbb{H}^{(i)} = \begin{bmatrix} \boldsymbol{h}^{(i)}(L)\boldsymbol{h}^{(i)}(L-1)\ldots\boldsymbol{h}^{(i)}(0) & \mathbf{0} & \ldots & \mathbf{0} \\ \mathbf{0} & \boldsymbol{h}^{(i)}(L) & \ldots\boldsymbol{h}^{(i)}(1)\,\boldsymbol{h}^{(i)}(0)\ldots & \mathbf{0} \\ \vdots & \vdots & \ddots\ \vdots\ \ \vdots & \ddots\ \vdots \\ \mathbf{0} & \mathbf{0} & \ldots\boldsymbol{h}^{(i)}(L)\boldsymbol{h}^{(i)}(L)\ldots\boldsymbol{h}^{(i)}(0) & \end{bmatrix} \tag{4.36}$$

that has the size of $PN_0\times(P+L)$ and $\bar{\boldsymbol{s}}_P^{(i)}(m) = [\bar{s}^{(i)}(mP+M-L)\ \cdots\ \bar{s}^{(i)}(mP+P+M-1)]^T$ for $i = 1,2,\cdots,N_i$; $m = 0,1,2,\cdots,I$ where $I = \lceil\frac{D-M}{P}\rceil$. The noise in this m^{th} subframe can be represented as $\boldsymbol{w}_P(m) = [\boldsymbol{n}^T(mP+M)\ \cdots\ \boldsymbol{n}^T(mP+P+M-1)]^T \in \mathbb{C}^{PN_0\times 1}$.

Then, $\boldsymbol{y}_P(m)$ can be written as

$$\begin{aligned} \boldsymbol{y}_P(m) &= \sum_{i=1}^{N_i}\mathbb{H}^{(i)}\bar{\boldsymbol{s}}_P^{(i)}(j)\ +\ \boldsymbol{w}_P(m) \\ &= \left[\mathbb{H}^{(1)}\ \mathbb{H}^{(2)}\ \cdots\ \mathbb{H}^{(N_i)}\right]\begin{bmatrix}\bar{\boldsymbol{s}}_P^{(1)}(m)\\ \bar{\boldsymbol{s}}_P^{(2)}(m)\\ \vdots \\ \bar{\boldsymbol{s}}_P^{(N_i)}(m)\end{bmatrix}\ +\ \boldsymbol{n}_P(m) \\ &= \mathbb{H}\bar{\boldsymbol{s}}_P(m)\ +\ \boldsymbol{n}_P(m) \end{aligned} \tag{4.37}$$

where $\mathbb{H} = \left[\mathbb{H}^{(1)}\ \mathbb{H}^{(2)}\ \cdots\ \mathbb{H}^{(N_i)}\right] \in \mathbb{C}^{PN_0\times N_i(P+L)}$, $\bar{\boldsymbol{s}}_P(m) = \left[(\bar{\boldsymbol{s}}_P^{(1)}(m))^T\ (\bar{\boldsymbol{s}}_P^{(2)}(m))^T\right.$

$\cdots\ (\bar{\boldsymbol{s}}_P^{(N_i)}(m))^T\big]$ and $\boldsymbol{n}_P(m) \sim \mathcal{CN}(0, \boldsymbol{\Sigma}')$ where $\boldsymbol{\Sigma}' = \boldsymbol{I}_P \otimes \boldsymbol{\Sigma}$.

Applying the idea of SD in colored Gaussian noise, we multiple (4.37) with $\boldsymbol{G}^{-1}$ where $\boldsymbol{G}\boldsymbol{G}^{\mathcal{H}} = \boldsymbol{\Sigma}'$ to yield

$$\begin{aligned} \boldsymbol{G}^{-1}\boldsymbol{y}_P(m) &= \boldsymbol{G}^{-1}\mathbb{H}\bar{\boldsymbol{m}}_P^{(i)}(j) + \boldsymbol{G}^{-1}\boldsymbol{n}_P(m) \\ \boldsymbol{y}_P^{'}(m) &= \mathbb{H}'\bar{\boldsymbol{s}}_P(m) \ + \ \boldsymbol{n}_P^{'}(m) \end{aligned} \tag{4.38}$$

In (4.38), $\boldsymbol{n}_P^{'}(m)$ is a white Gaussian random vector, therefore we can apply SD described in Chapter 3 to find the ML solution to $\bar{\boldsymbol{s}}_P(m)$ after translating (4.38) into its real-equivalent form.

Note that in (4.37), the matrix $\mathbb{H}$ has the size of $PN_0 \times N_i(P+L)$. In order to apply the SD algorithm, it is required that the number of rows should not be less than the number of columns, i.e.,

$$\begin{aligned} PN_0 &\geq N_i(P+L) \\ \text{or} \qquad N_0 &\geq N_i(1+\frac{L}{P}). \end{aligned} \tag{4.39}$$

Therefore, in general, the number of receive antennas should be greater than the number of transmit antennas.

4.4 Channel estimation and detection for flat fast fading channels

4.4.1 Sytem model

We still consider a MIMO system having N_i transmitters and N_0 receivers. Each link in our system is assumed to be flat fading channel with Doppler spread effects taken into account. Therefore, the received signals are simply the transmitted signals faded by a time-varying stochastic process. More explicitly,

the Rayleigh distribution is used to describe the statistical time-varying nature of received signal envelop due to flat fading and the received signal phase is assumed to be uniformly distributed over interval of $[0, 2\pi)$.

The Jakes' simulation model [26] is a statistical model that can be used for the channel where the envelope fluctuation is characterized by Rayleigh process. The Rayleigh process, $\zeta(t)$ is obtained from the envelope of a narrow-band complex Gaussian random process

$$\mu(t) = \mu_1(t) + j\mu_2(t) \tag{4.40}$$

where $\mu_1(t)$ and $\mu_2(t)$ are uncorrelated real Gaussian random processes with zero-mean, $E\{\mu_i(t)\} = 0$, and equal variance $E\{\mu_i^2(t)\} = \sigma_{\mu_i}^2 = \sigma_0^2/2$, $i = 1, 2$. Thus,

$$\zeta(t) = |\mu(t)| = \sqrt{\mu_1^2(t) + \mu_2^2(t)} \tag{4.41}$$

is a Rayleigh distributed random process. The power spectrum density of the two Gaussian random process, which are widely accepted Jakes' power spectrum, are written as

$$S_{\mu_i\mu_i}(f) = \begin{cases} \frac{\sigma_0^2/2}{\pi f_{max}\sqrt{1-(f/f_{max})^2}} & |f| < f_{max} \\ 0 & elsewhere \end{cases}, i = 1, 2 \tag{4.42}$$

where f_{max} the the maximum Doppler shift [2]. By taking the inverse Fourier transform of (4.42), the autocorrelation function of $\mu_i(t), i = 1, 2$ is given by

$$r_{\mu_i\mu_i}(\tau) = \frac{\sigma_0^2}{2} J_0(2\pi f_{max}\tau) \tag{4.43}$$

[2]The Doppler shift (Doppler frequency) of an elementary wave is equlal to $f = f_{max}\cos\alpha$, where α is the angle of arrival and $f_{max} = vf_0/c_0$ denotes the maximum Doppler frequency(v: velocity of user, f_0: carrier frequency, c_0: speed of light)

The power spectrum density of $\mu(t)$ is thus

$$S_{\mu\mu}(f) = S_{\mu_1\mu_1}(f) + S_{\mu_2\mu_2}(f) = \begin{cases} \frac{\sigma_0^2}{\pi f_{max}\sqrt{1-(f/f_{max})^2}} & |f| < f_{max} \\ 0 & elsewhere \end{cases} \tag{4.44}$$

and its autocorrelation function is

$$r_{\mu\mu}(\tau) = r_{\mu_1\mu_1}(\tau) + r_{\mu_2\mu_2}(\tau) = \sigma_0^2 J_0(2\pi f_{max}\tau). \tag{4.45}$$

We consider the link from i^{th} transmitter to j^{th} receiver in our MIMO system. The received signal in continuous-time domain is

$$y^{(j)}(t) = h_{i,j}(t)s^{(i)}(t) + w^{(j)}(t) \tag{4.46}$$

where the random process $h_{i,j}(t)$ has the power spectrum density of (4.44) and the autocorrelation of (4.45).

Therefore, the discrete-time form of (4.46) can be written as

$$y^{(j)}(k) = h_{i,j}(k)s^{(i)}(k) + w^{(j)}(k), \quad k = \cdots, 0, 1, 2, \cdots \tag{4.47}$$

The sequence $\{h_{i,j}(k)\}_{k=-\infty}^{+\infty}$ has the autocorrelation function that is the sampled function of (4.45) at period of T, i.e.,

$$r_{h^{(i,j)}h^{(i,j)}}(m) = \sigma_0^2 J_0(2\pi f_{max} T m), \quad m = \cdots, 0, 1, 2, \cdots \tag{4.48}$$

For our MIMO system, the received signals from N_0 receivers at time k are grouped to form a matrix $\boldsymbol{y}(k)$ that is expressed as

$$\begin{bmatrix} y^{(1)}(k) \\ y^{(2)}(k) \\ \vdots \\ y^{(N_0)}(k) \end{bmatrix} = \begin{bmatrix} h_{1,1}(k) \cdots\cdots h_{N_i,1}(k) \\ h_{1,2}(k) \cdots\cdots h_{N_i,1}(k) \\ \vdots \quad \vdots \ddots \quad \vdots \\ h_{1,N_0}(k) \cdots\cdots h_{N_i,N_0}(k) \end{bmatrix} \begin{bmatrix} s^{(1)}(k) \\ s^{(2)}(k) \\ \vdots \\ s^{(N_i)}(k) \end{bmatrix} + \begin{bmatrix} w^{(1)}(k) \\ w^{(2)}(k) \\ \vdots \\ w^{(N_0)}(k) \end{bmatrix}$$

or

$$\boldsymbol{y}(k) = \boldsymbol{H}(k)\boldsymbol{s}(k) + \boldsymbol{w}(k) \tag{4.49}$$

where $y^{(j)}(k)$, $s^{(i)}(k)$, $w^{(j)}(k)$ is the signal received by the j^{th} receiver, signal transmitted by the i^{th} transmitter, additive noise at the j^{th} receiver at time k, respectively. $h_{i,j}(k)$ is the channel coefficient from i^{th} transmitter to j^{th} receiver at time k, $i = 1, 2, \cdots, N_i$, $j = 1, 2, \cdots, N_0$. $\boldsymbol{y}(k) \in \mathbb{C}^{N_0 \times 1}$, $\boldsymbol{s}(k) \in \mathcal{C}^{N_i \times 1}$, $\boldsymbol{w}(k) \in \mathbb{C}^{N_0 \times 1}$ and $\boldsymbol{H}(k) \in \mathbb{C}^{N_0 \times N_i}$. The noise at the receivers are assume to be temporally white but dependent among the receivers, i.e., $E\left\{\boldsymbol{w}(t_1)\boldsymbol{w}(t_2)^{\mathcal{H}}\right\} = \boldsymbol{\Sigma} \times \delta(t_1 - t_2)$ where $\boldsymbol{\Sigma}$ is a $N_0 \times N_0$ matrix to be determined.

The symbol structure from a transmitter is similar to that in case of quasi-static flat fading channels, i.e., symbols are grouped into blocks of N symbols in which the first M symbols are pilot symbols.

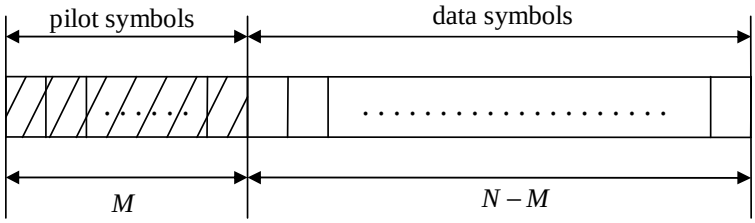

Figure 4.3: Symbols structure for fast fading channels.

The per-antenna SNR in this case is determined as

$$\text{SNR} = \frac{P_s \sigma_0^2}{\sigma_w^2}. \tag{4.50}$$

where σ_w^2 is the variance of noise at each receiver.

4.4.2 Channel estimation

For our analysis of the estimation algorithm, we assume that the channel remains almost unchanged within a block of N symbols. Hence, the channel

matrix is approximated as time invariant so that the input-output relationship can be writtens as

$$\boldsymbol{y}(k) = \boldsymbol{H}\boldsymbol{s}(k) + \boldsymbol{w}(k), \quad k = 0, 2, \cdots, M-1. \tag{4.51}$$

Our assumption can be applied when the value of $f_{max}T$ is small and the value of N is small. If we group M received signal vectors corresponding to M pilot symbols to form $\boldsymbol{Y} = [\boldsymbol{y}(0)\ \boldsymbol{y}(1)\ \cdots\ \boldsymbol{y}(M-1)] \in \mathbb{C}^{N_0 \times M}$ then

$$\boldsymbol{Y} = \boldsymbol{H}\boldsymbol{S} + \boldsymbol{W} \tag{4.52}$$

where $\boldsymbol{S} = [\boldsymbol{s}(0)\ \boldsymbol{s}(1)\ \cdots\ \boldsymbol{s}(M-1)]$ and $\boldsymbol{W} = [\boldsymbol{w}(0)\ \boldsymbol{w}(1)\ \cdots\ \boldsymbol{w}(M-1)] \in \mathbb{C}^{N_0 \times M}$.

From the DEML estimator of section 4.1, the estimation of $\boldsymbol{H}$ and $\boldsymbol{\Sigma}$ are

$$\begin{aligned} \hat{\boldsymbol{H}} &= \hat{\boldsymbol{R}}_{\boldsymbol{SY}}^{\mathcal{H}} \hat{\boldsymbol{R}}_{\boldsymbol{SS}}^{-1} \\ \hat{\boldsymbol{\Sigma}} &= \hat{\boldsymbol{R}}_{\boldsymbol{YY}} - \hat{\boldsymbol{R}}_{\boldsymbol{SY}}^{\mathcal{H}} \hat{\boldsymbol{R}}_{\boldsymbol{SS}}^{-1} \hat{\boldsymbol{R}}_{\boldsymbol{SY}} \end{aligned} \tag{4.53}$$

where $\hat{\boldsymbol{R}}_{\boldsymbol{YY}} = \frac{1}{M}\boldsymbol{Y}\boldsymbol{Y}^{\mathcal{H}}$, $\hat{\boldsymbol{R}}_{\boldsymbol{SY}} = \frac{1}{M}\boldsymbol{S}\boldsymbol{Y}^{\mathcal{H}}$, $\hat{\boldsymbol{R}}_{\boldsymbol{SS}} = \frac{1}{M}\boldsymbol{S}\boldsymbol{S}^{\mathcal{H}}$.

4.4.3 Symbol detection

In this section, the estimated value of $\boldsymbol{H}$ and $\boldsymbol{\Sigma}$ are used in SD to decode the transmitted signals during the left $N - M$ symbol periods. In every equation form now on, we assume $\boldsymbol{H}$ and $\boldsymbol{\Sigma}$ have been estimated by DEML algorithm.

At any k instant, $k = M, M+1, \cdots, N-1$, the received signal vector is

$$\boldsymbol{y}(k) = \boldsymbol{H}\boldsymbol{s}(k) + \boldsymbol{w}(k) \tag{4.54}$$

Equation (4.54) is post-multiplied with $\boldsymbol{G}^{-1}$ where $\boldsymbol{G}\boldsymbol{G}^{\mathcal{H}} = \boldsymbol{\Sigma}$ to form

$$\begin{aligned} \boldsymbol{G}^{-1}\boldsymbol{y}(k) &= \boldsymbol{G}^{-1}\boldsymbol{H}\boldsymbol{s}(k) + \boldsymbol{G}^{-1}\boldsymbol{w}(k) \\ \boldsymbol{y}'(k) &= \boldsymbol{H}'\boldsymbol{s}(k) + \boldsymbol{w}'(k) \end{aligned} \tag{4.55}$$

and SD is applied in (4.55) (after transforming to its real-equivalent form) to find the ML estimation of transmitted symbol vector $\boldsymbol{s}(k)$ at time k.

4.5 Summary

In this Chapter, we consider three realizations of the general MIMO system model that are developed in Chapter 2: quasi-static flat fading channels, quasi-static frequency selective fading channels and flat fast fading channel. The system model is presented for each case. The organization of symbols at each transmitter is also addressed. For every case, symbols are grouped into blocks in which several leading symbols served as pilot symbols to estimate the channel information needed in the detection process. For the fast fading case, we have assumed block fading for blocks of very short lengths as an approximate analysis. The validity of this assumption is verified by computer simulated results in Section 5.3.

CHAPTER 5

RESULTS AND DISCUSSIONS

In this chapter, we present computer simulated results on the performance of the channel information estimation and decoding algorithms proposed.

We assume that the noise vector $\boldsymbol{w}(k)$ at any time instance k at N_0 receivers has the covariance matrix $\boldsymbol{\Sigma}$ whose $(m,n)^{th}$ element is

$$\boldsymbol{\Sigma}_{m,n} = \sigma_w^2.(0.9)^{|m-n|}.\exp\left[j\left(\frac{\pi}{2}\right)(m-n)\right],\ 1 \leq m,n \leq N_0$$

i.e., colored noise.This noise covariance model was adopted in [8]. The matrix $\boldsymbol{\Sigma}$ can also be written as $\boldsymbol{\Sigma} = \sigma_w^2\boldsymbol{\Sigma}_0$ where

$$(\boldsymbol{\Sigma}_0)_{m,n} = (0.9)^{|m-n|}.\exp\left[j\left(\frac{\pi}{2}\right)(m-n)\right],\ 1 \leq m,n \leq N_0$$

Besides, we also consider the white noise case in which the $\boldsymbol{\Sigma} = \sigma_w^2\boldsymbol{I}_{N_0}$.

For the purpose of comparisons, we also obtained simulated results using the Zero-Forcing (ZF) detection method. ZF is a classical detection technique which is used widely in communication systems, and is briefly summarized below.

For the model

$$\boldsymbol{y} = \boldsymbol{H}\boldsymbol{s} + \boldsymbol{w}, \tag{5.1}$$

the unconstrained least-squares result is

$$\hat{\boldsymbol{s}} = \boldsymbol{H}^{\dagger}\boldsymbol{y}, \tag{5.2}$$

where $\boldsymbol{H}^{\dagger} = (\boldsymbol{H}^{\mathcal{H}}\boldsymbol{H})^{-1}\boldsymbol{H}^{\mathcal{H}}$ is called the pseudo-inverse of $\boldsymbol{H}$. The entries of $\hat{\boldsymbol{s}}$ are not necessarily the elements used in the signal constellation. Rounding them off to the closest elements of constellation (a process referred as slicing) provides the estimated value of $\boldsymbol{s}$ according to the ZF algorithm.

5.1 Quasi-static flat fading channels

In Figure 5.1, we present BER versus SNR for the MIMO system having $N_i = 2$ transmitters and $N_0 = 2$ receivers in the colored noise environment. We assume the channels from transmitters to receivers are independent. At any time instance, a link in our system is modeled as a complex Gaussian random variable with zero mean, i.e., there are no LOS paths in our system. We assume that the channel coefficients remain unchanged over a interval of $N = 44$ symbols in which the first $M = 4$ symbols are pilot symbols used to estimate the channel coefficients and the noise covariance matrix. From Figure 5.1, we see that SD using the channel information from DEML estimator outperforms the ZF with perfect CSI.

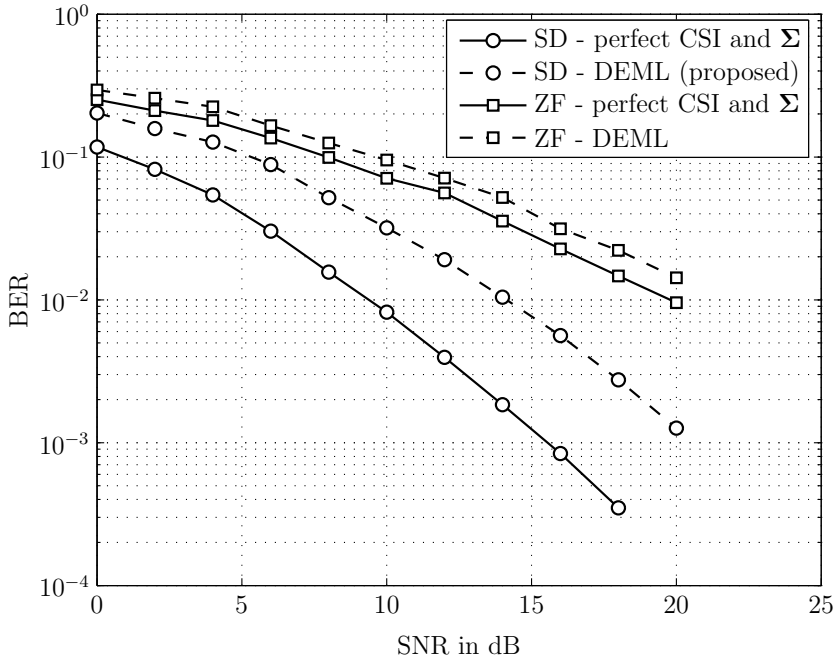

Figure 5.1: BER v.s. SNR for $N = 44$, $M = 4$, no LOS's and in the colored noise environment.

For example, at a BER of 10^{-2}, the former outperforms the latter by more

than 5 dB.

Further, the results also show that the performance of the ZF algorithm using the channel information obtained from the DEML estimator is only about 1dB poorer when compared to the case with perfect channel information. This observation illustrates the accuracy of channel information obtained by our proposed estimator.

It is also seen in the Figure 5.1 that the loss of the SD using the channel information from the DEML estimator and the SD using perfect channel information is around 5dB. This loss is larger than that of the ZF algrithm using information from DEML estimator compared with the ZF algorithm using perfect channel information. We can infer that the SD is more sensitive with channel information estimation error than the ZF algorithm.

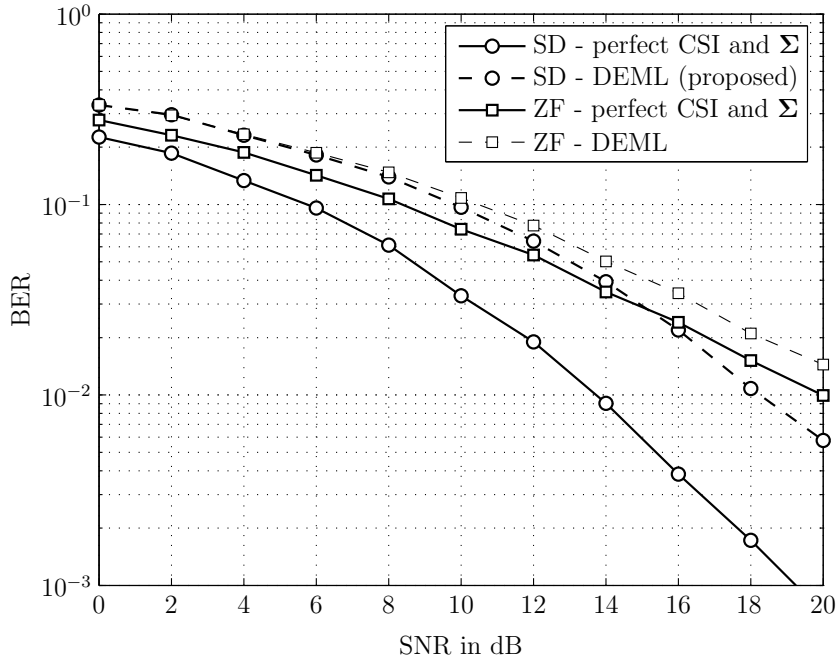

Figure 5.2: BER v.s. SNR for $N = 44$, $M = 4$, no LOS's and in the white noise environment.

In Figure 5.2, the BER performance for the same system as above but op-

erating in a white noise environment is presented. We see that for the case of white noise, the proposed method only outperforms the ZF with perfect CSI and noise covariance matrix when the SNR is above around 15 dB. From this SNR value, the gap between them becomes larger. Comparing with the case of colored noise, at the BER of 10^{-2}, the case for colored noise outperforms that for white noise by more than 2 dB.

We next consider the same system but there is a LOS path in each link in the system. Figure 5.3 shows us the performance with the Ricean factor of $K = 2$ in the colored noise environment and Figure 5.4 in the white noise environment, respectively.

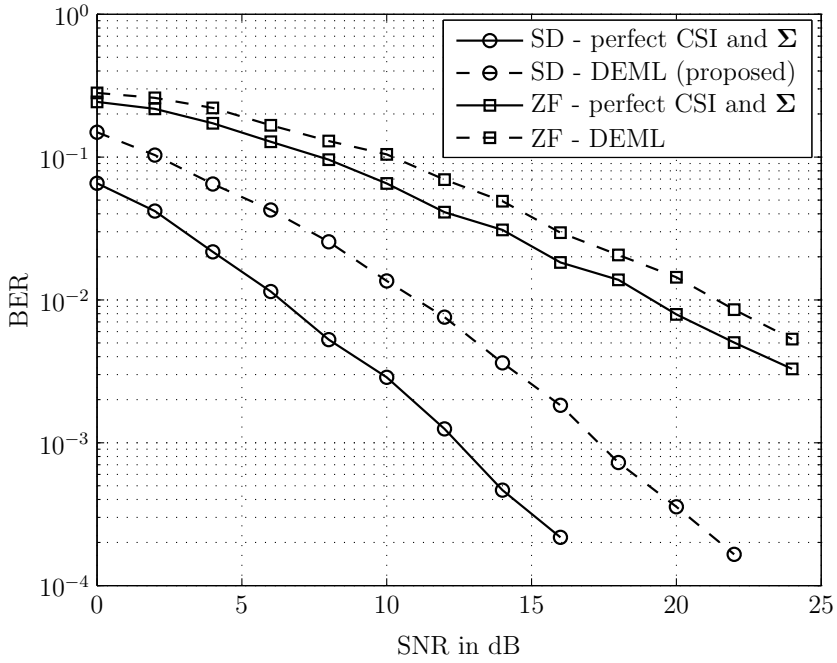

Figure 5.3: BER v.s. SNR for $N = 44$, $M = 4$. Ricean factor of $K = 2$ and in the colored noise environment.

In this case, at BER $= 10^{-2}$, the SNR loss of the ZF using perfect channel information to the SD using the channel information from DEML estimator in the colored noise environment is around 10dB and in the white noise environment

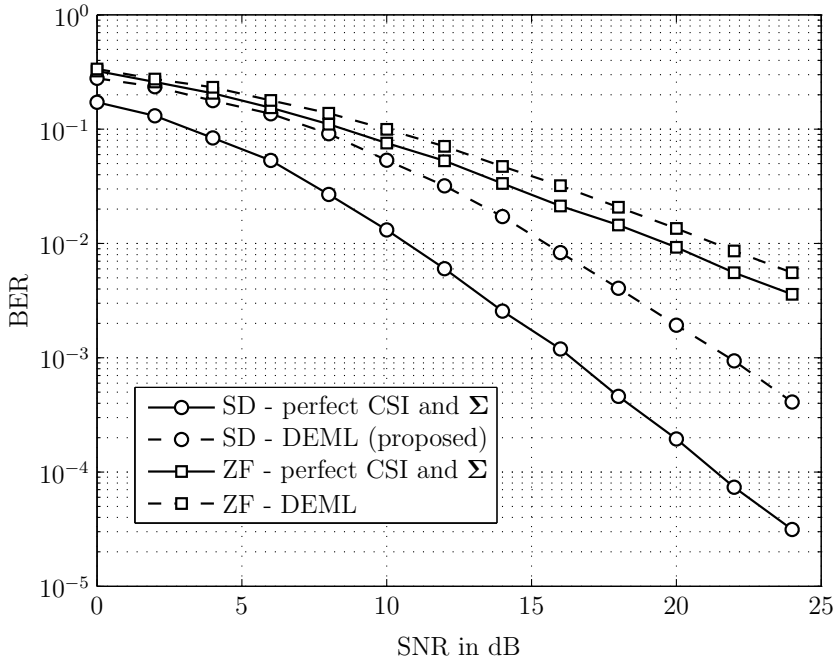

Figure 5.4: BER v.s. SNR for $N = 44$, $M = 4$. Ricean factor of $K = 2$ and in the colored noise environment

is around 4 dB, which are larger than that of without LOS paths.

To examine the accuracy of our approach, we plotted the average MSE of the channel coefficient in case of colored and white noise environments in Figure 5.5 and Figure 5.6, respectively. The MSE of the noise covariance estimates are plotted in Figure 5.7 and Figure 5.8 for the colored and white noise environments, respectively. We observe that the MSE's decrease rapidly with the increase of SNR. It is further observed that at low SNR, the MSE incurred is much larger for the case when a LOS component is present.

Figure 5.9 illustrates the BER as a function of SNR for the 2×2 system in both the colored and white noise environments, without LOS. Figure 5.10 presents the BER of the same system in the presence of an LOS path.

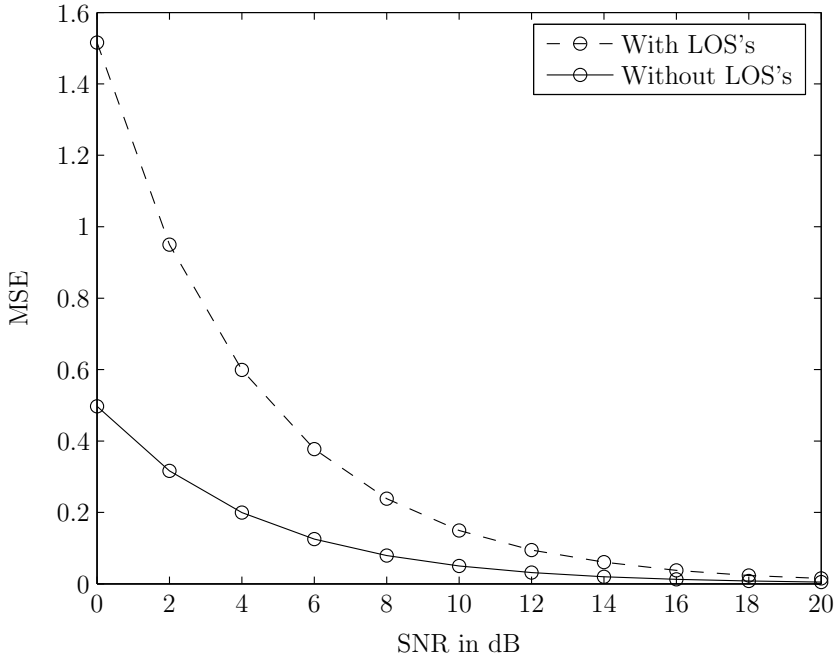

Figure 5.5: Average MSE of channel coefficients in 2×2 flat fading system, $N = 44$ and $M = 4$, with and without LOS's in the colored noise environment.

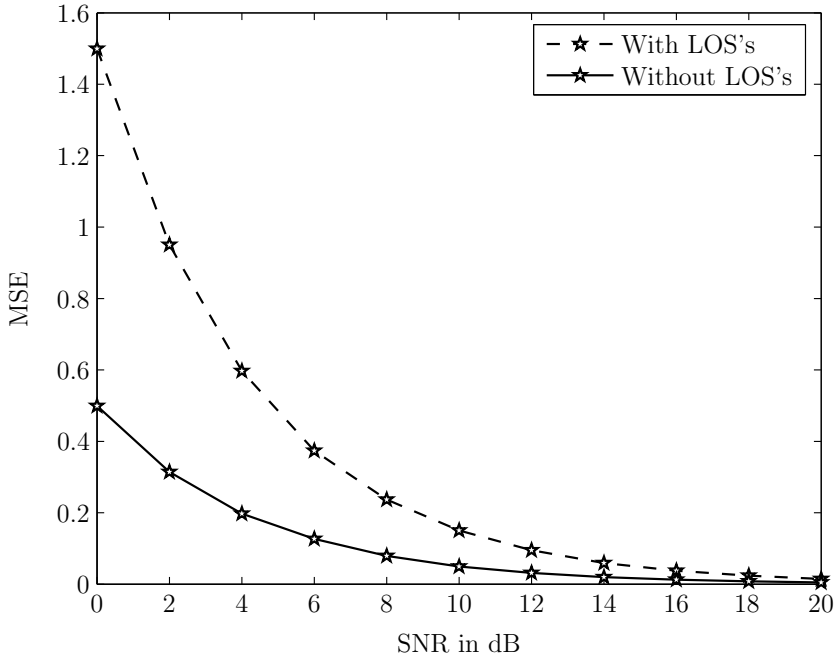

Figure 5.6: Average MSE of channel coefficients in 2×2 flat fading system, $N = 44$ and $M = 4$, with and without LOS's in the white noise environment.

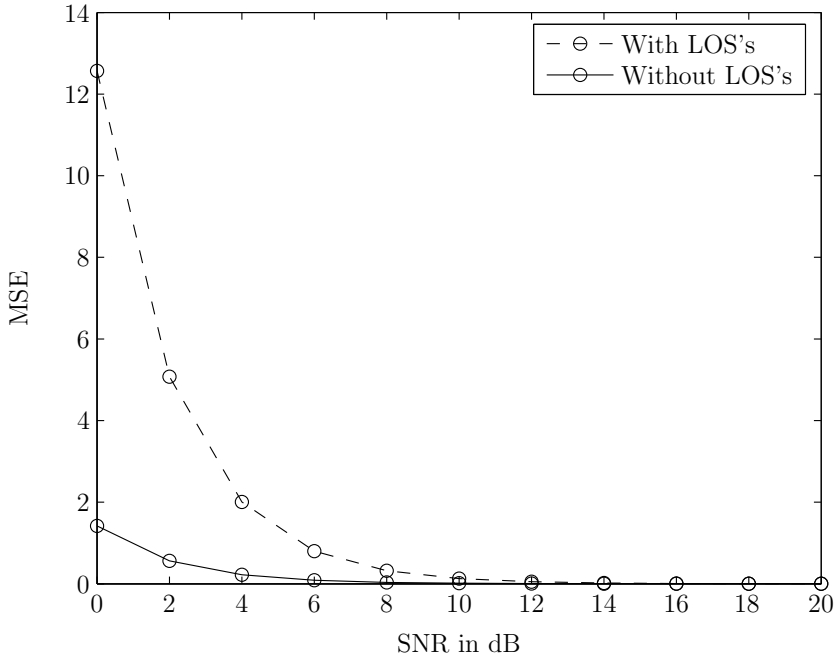

Figure 5.7: Average MSE of elements of $\mathbf{\Sigma}$ in 2×2 flat fading system, $N = 44$ and $M = 4$, with and without LOS's in the colored noise environment.

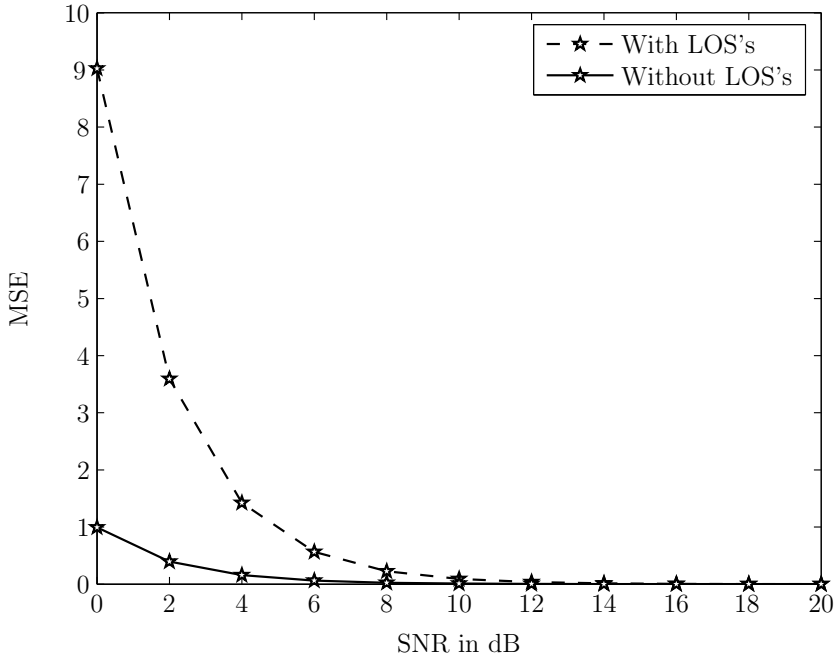

Figure 5.8: Average MSE of elements of $\mathbf{\Sigma}$ in 2×2 flat fading system, $N = 44$ and $M = 4$, with and without LOS's in the white noise environment

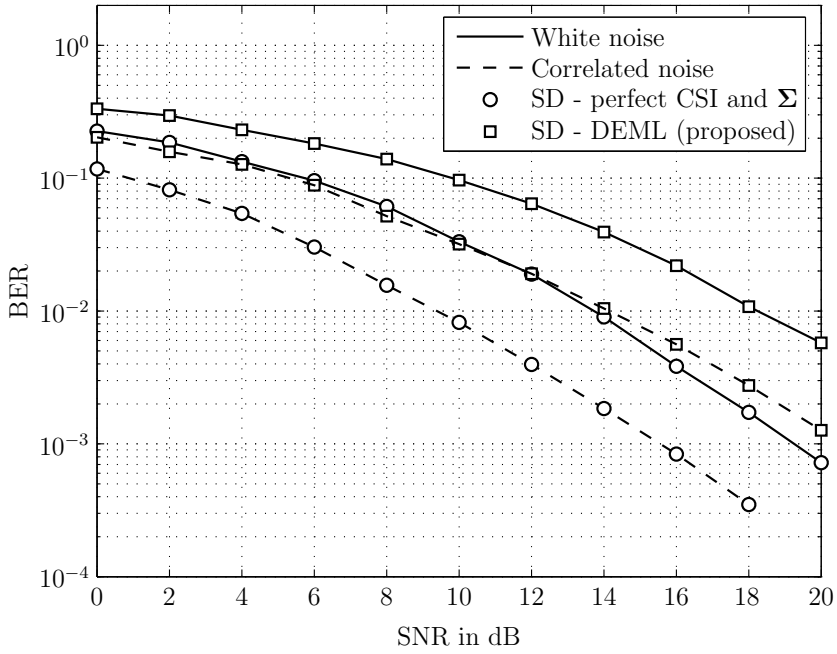

Figure 5.9: BER v.s. SNR for the 2×2 flat fading system, $N = 44$ and $M = 4$, without LOS's in the colored and white noise environments.

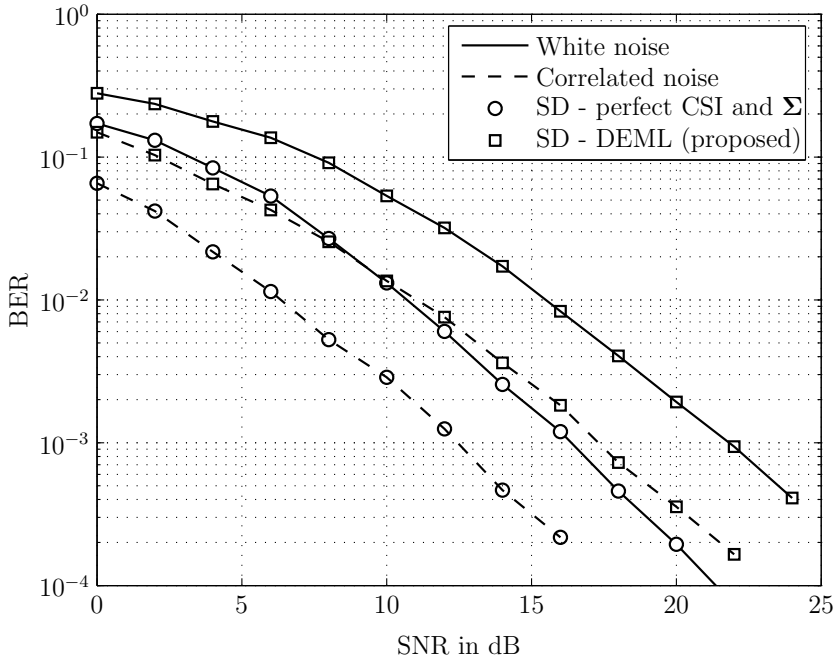

Figure 5.10: BER v.s. SNR for the 2×2 flat fading system, $N = 44$ and $M = 4$, with LOS's in the colored and white noise environments.

From the two Figures, we see that the performance of the system in the colored noise environment is better that that in the white noise environment.

To explain this phenomenon, we resort to the Matched-Filter Bound (MFB) [27]. For the system of

$$\begin{aligned} \boldsymbol{y} &= \boldsymbol{H}\boldsymbol{s} + \boldsymbol{w} \\ &= [\boldsymbol{h}_1\ \boldsymbol{h}_2\ \ \boldsymbol{h}_i\ \cdots\ \boldsymbol{h}_{N_i}] \begin{bmatrix} s^{(1)} \\ s^{(2)} \\ \vdots \\ s^{(N_i)} \end{bmatrix} + \boldsymbol{w} \end{aligned} \tag{5.3}$$

where $E\left\{\boldsymbol{w}\boldsymbol{w}^{\mathcal{H}}\right\} = \sigma_w^2 \boldsymbol{I}_{N_0}$ (i.e., white noise environment), the SNR for the i^{th} symbol according to MFB is [pg. 448, 27]:

$$SNR_{MFB,i,white\ noise} = \frac{\|\boldsymbol{h}_i\|^2}{\sigma_w^2}. \tag{5.4}$$

For the colored noise environment, the covariance matrix of $\boldsymbol{w}$ is $\boldsymbol{\Sigma} = E\left\{\boldsymbol{w}\boldsymbol{w}^{\mathcal{H}}\right\} = \sigma_w^2 \boldsymbol{\Sigma}_0$. The Cholesky decomposition of $\boldsymbol{\Sigma}_0$ is $\boldsymbol{\Sigma}_0 = \boldsymbol{G}_0^{\mathcal{H}} \boldsymbol{G}_0$ and the Cholesly decompostion of $\boldsymbol{\Sigma}$ can be easily written as $\boldsymbol{\Sigma} = \sqrt{\sigma_w^2}\boldsymbol{G}_0^{\mathcal{H}} \sqrt{\sigma_w^2}\boldsymbol{G}_0$. The whitening operation is accomplished by post-multiplying (5.3) by $(\sqrt{\sigma_w^2}\boldsymbol{G}_0^{\mathcal{H}})^{-1}$ as follows:

$$\underbrace{(\sqrt{\sigma_w^2}\boldsymbol{G}_0^{\mathcal{H}})^{-1}\boldsymbol{y}}_{\boldsymbol{y}'} = \underbrace{(\sqrt{\sigma_w^2}\boldsymbol{G}_0^{\mathcal{H}})^{-1}\boldsymbol{H}}_{\boldsymbol{H}'=[\boldsymbol{h}_1'\cdots\boldsymbol{h}_i'\cdots\boldsymbol{h}_{N_i}']}\boldsymbol{s} + \underbrace{(\sqrt{\sigma_w^2}\boldsymbol{G}_0^{\mathcal{H}})^{-1}\boldsymbol{w}}_{\boldsymbol{w}'}. \tag{5.5}$$

It is straightforward to prove that the $E\left\{\boldsymbol{w}'(\boldsymbol{w}')^{\mathcal{H}}\right\} = \boldsymbol{I}_{N_0}$. Therefore, the SNR for the i^{th} symbol according to the MFB for the colored noise case is:

$$SNR_{MFB,i,colored\ noise} = \frac{\|\boldsymbol{h}_i'\|^2}{1} = \frac{\|(\boldsymbol{G}_0^{\mathcal{H}})^{-1}\boldsymbol{h}_i\|^2}{\sigma_w^2}. \tag{5.6}$$

In Figure 5.11, the 2×2 system is investigated and the $SNR_{MFB,i}$'s are presented for both colored and white noise environments. From the Figure we

see that for the colored noise environment, $SNR_{MFB,i}$ is larger than that of the white noise environment. Hence, the performance of the system in the colored noise environment is better than that of the white noise.

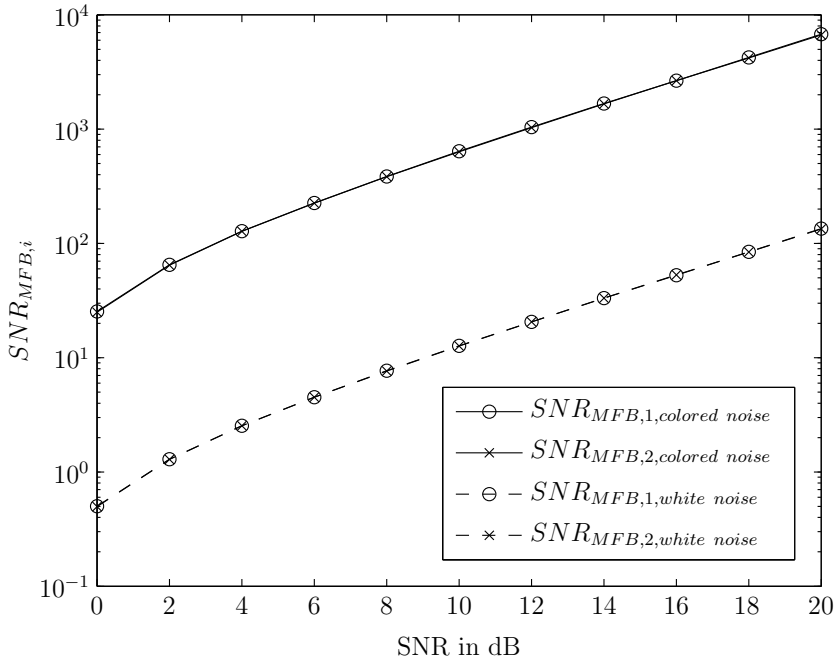

Figure 5.11: Compare the $SNR_{MFB,i}$ for 2×2 systems in the colored and white noise environments.

5.2 Quasi-static frequency selective fading channels

In this section, we consider a system with $N_i = 1$ transmitter and $N_0 = 2$ receivers. The channels between the transmitter and receivers are modeled as FIR dispersive channels with $L = 1$, i.e., each channel has two taps in its impulse response, which is basically the two-ray model.

First of all, we assume that the channels are independent. Further, we also assume that in our system there is no LOS path between the transmitter and receivers so that each tap of any channel impulse response can be modeled as a complex Gaussian random variable with zero mean and a common variance.

We consider a frame structure in which the frame length is $N = 44$, the first $M = 4$ symbols are used to estimated the channel coefficients and the noise covariance matrix. Figure 5.12 and Figure 5.13 present the average Mean Square Error (MSE) of each tap in the system in the colored and white noise environments, respectively.

Figure 5.14 and Figure 5.15 illustrate the average MSE of elements of $\mathbf{\Sigma}$ in the colored and white noise environments, respectively. We observe that the average MSE for both noise environments decreases exponentially as SNR increases.

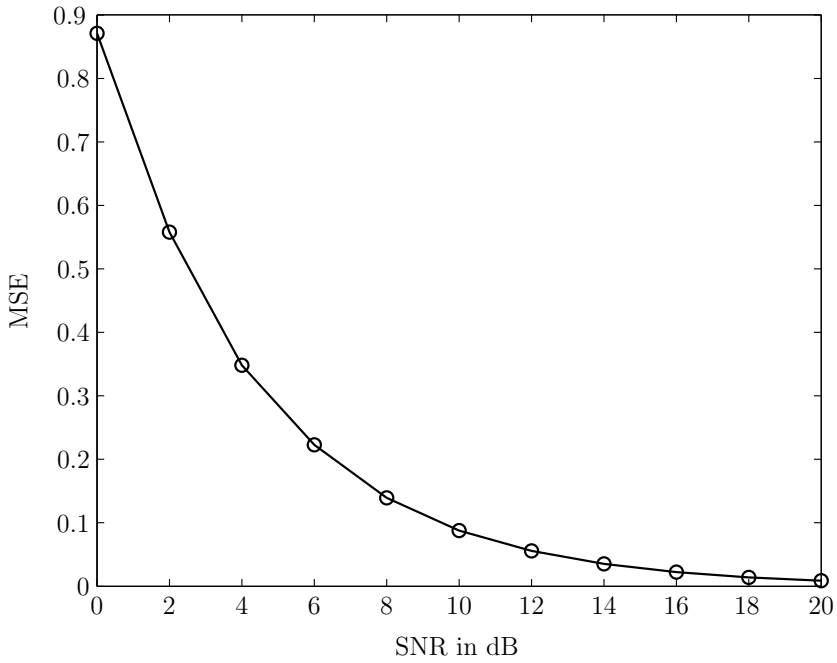

Figure 5.12: Average MSE of each channel coefficients, without LOS paths, in the colored noise environment.

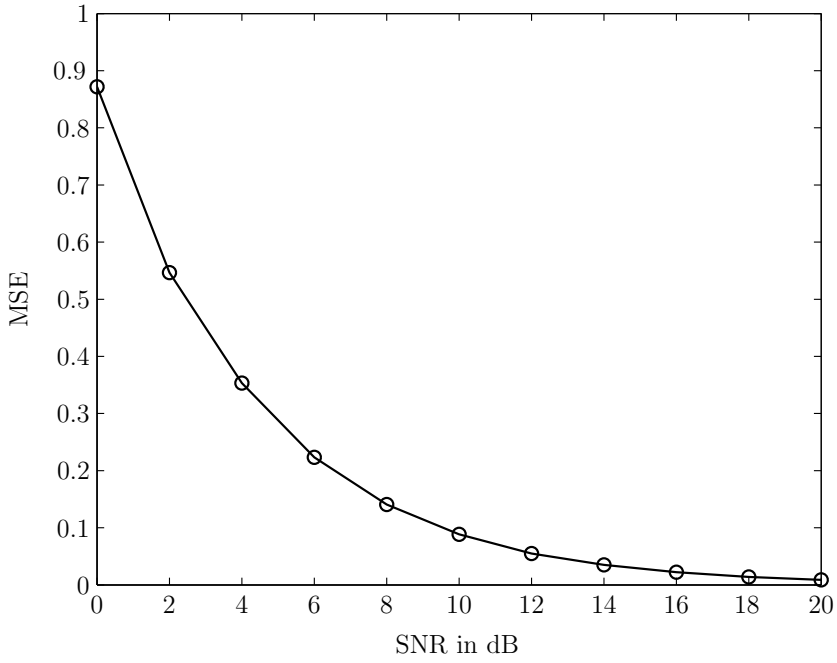

Figure 5.13: Average MSE of each channel coefficients, without LOS paths, in the white noise environment.

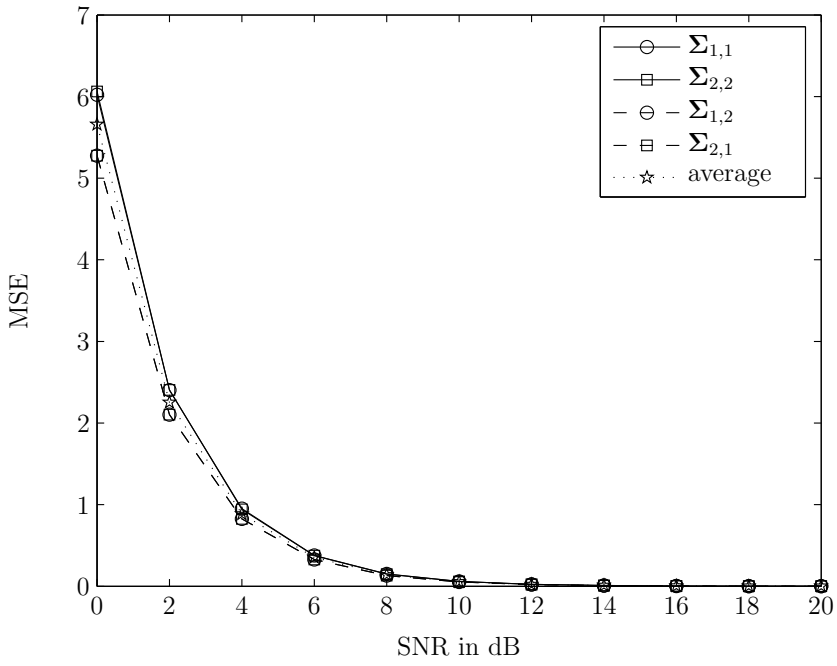

Figure 5.14: Average MSE of elements of $\mathbf{\Sigma}$, without LOS paths, in the colored noise environment.

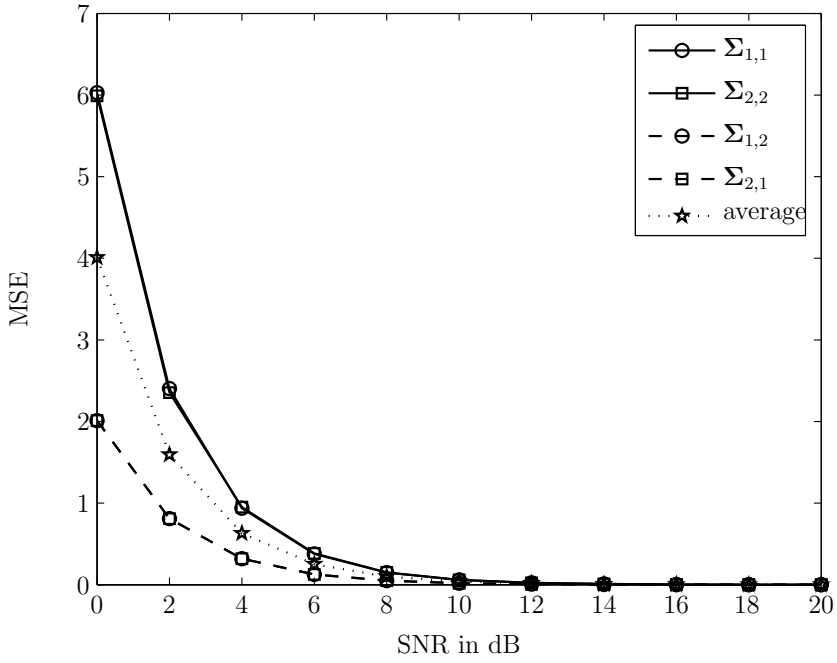

Figure 5.15: Average MSE of elements of $\mathbf{\Sigma}$, without LOS paths, in the white noise environment.

In Figure 5.16 and Figure 5.17, the BER as a function of SNR is shown for the cases of colored and white noise, respectively.

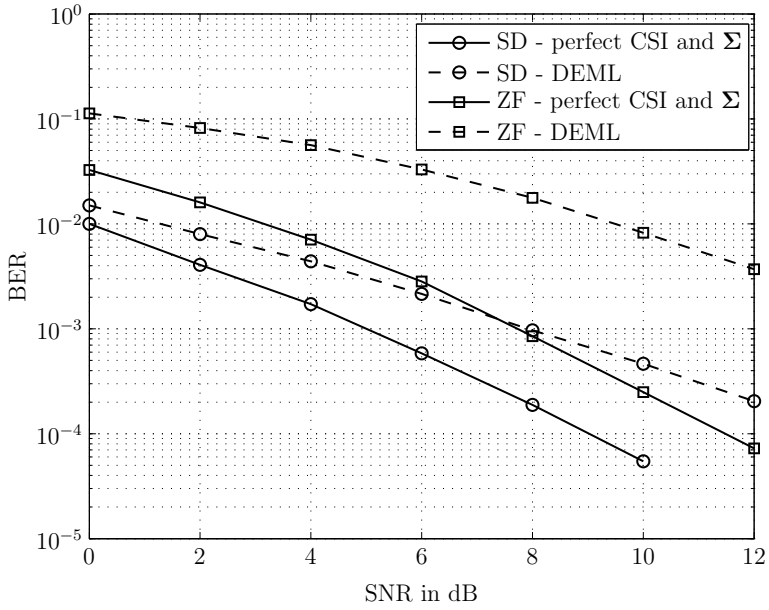

Figure 5.16: BER v.s. SNR for $N = 44, M = 4$, without LOS paths, in the colored noise environment.

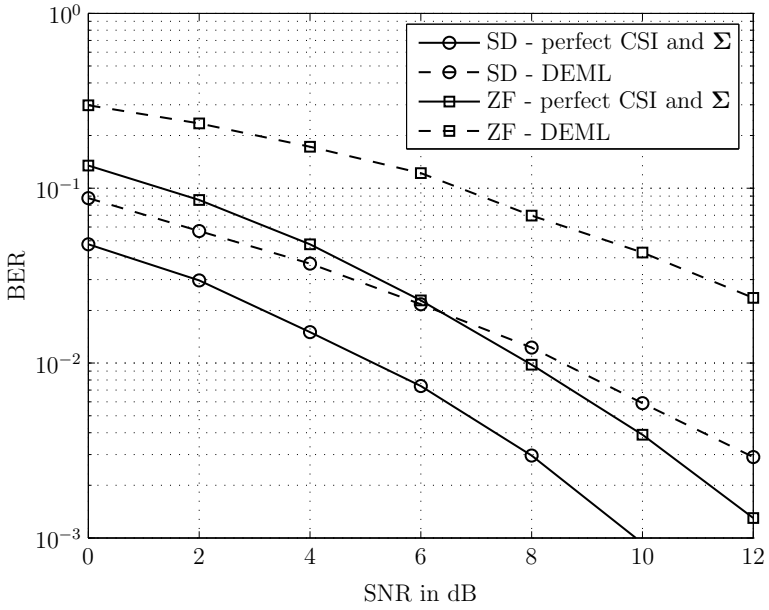

Figure 5.17: BER v.s. SNR for $N = 44, M = 4$, without LOS paths, in the white noise environment.

As can be seen from Figure 5.16 for the colored noise case, by applying DEML estimator to estimate channel information and using the estimated information to perform SD, the proposed system performs better than ZF with known CSI and noise covariance when SNR is below about 7 dB. For the white noise case, Figure 5.17 shows that the proposed method outperforms the ZF with known CSI and noise covariance when SNR is below about 6 dB.

With the same 1×2 system above, in Figure 5.18, we present the BER for two cases in the colored noise environment: the first one $N = 44,\ M = 4$ and the second one is $N = 24,\ M = 4$, i.e., the number of pilot symbols equals 4 in each case, the first case has 40 data symbols compared to the second case which has only 20 data symbols.

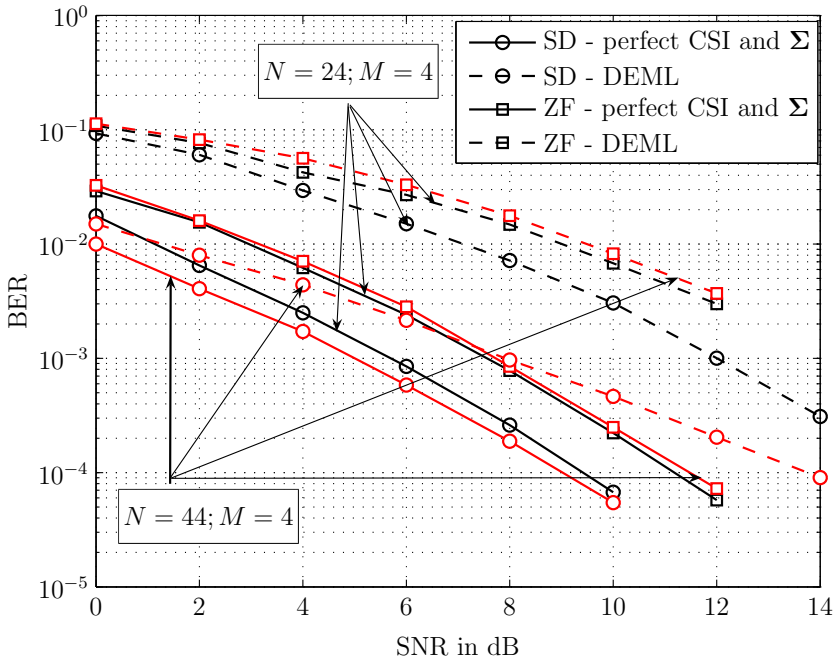

Figure 5.18: BER v.s. SNR for $N = 44, M = 4$ and $N = 24, M = 4$, without LOS paths, in the colored noise environment.

The same investigation is repeated for the white noise case and the results are shown in Figure 5.19.

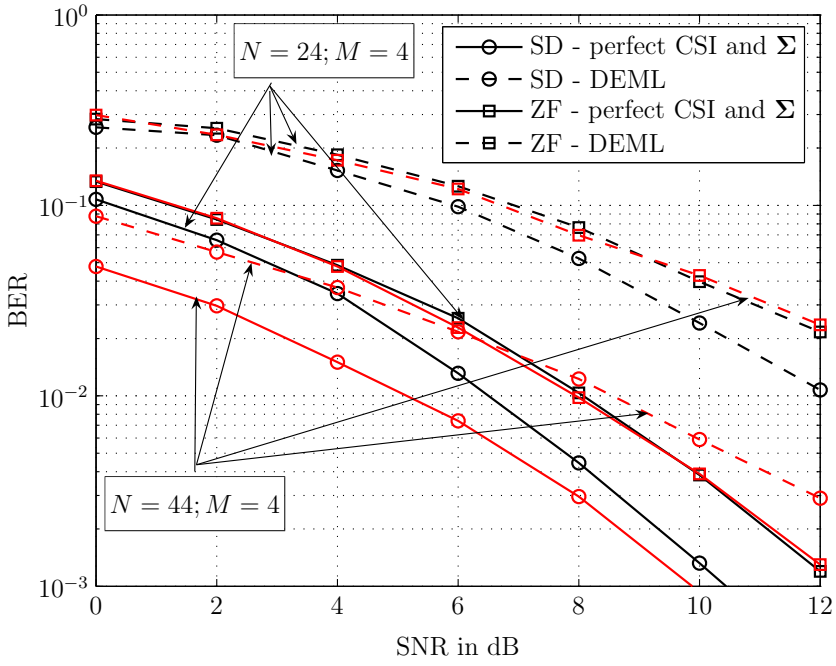

Figure 5.19: BER v.s. SNR for $N = 44, M = 4$ and $N = 24, M = 4$, without LOS paths, in the white noise environment.

When SD (using the channel information from DEML estimator) is applied, we observe that better performance can be achieved by using a frame constructed with larger number of data symbols and this observation is applied for both noise environments.

In Figure 5.20, we present a comparison of the two noise environments in term of BER as a function of SNR. It can be seen from the figure that the performance in the colored noise environment outperforms that of the white noise environment. This observation also happens for the quasi-static flat fading case as in Section 5.2. The observation can also be explained by using the arguments given in Section 5.2.

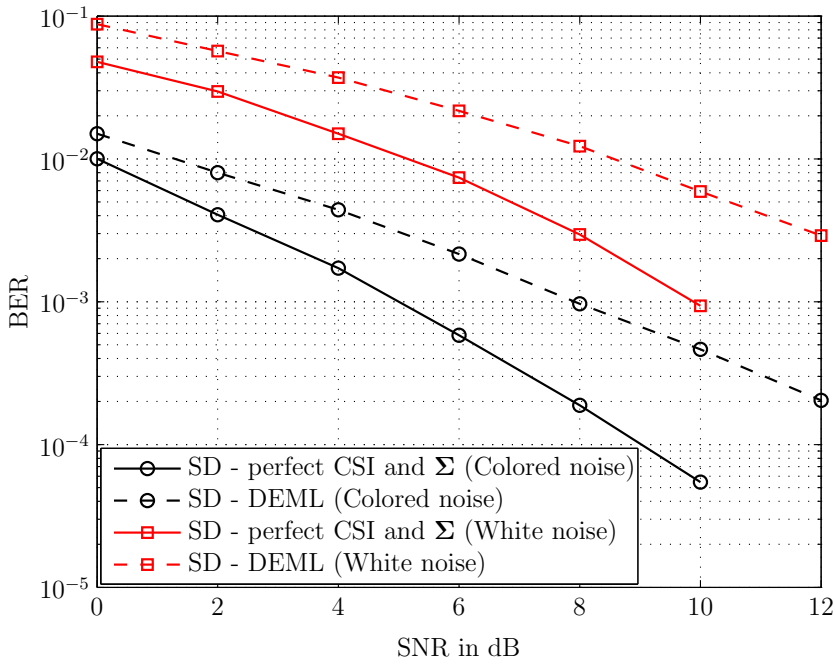

Figure 5.20: BER v.s. SNR for $N = 44, M = 4$, without LOS paths, in the colored and white noise environment.

In the presence of LOS's, the first tap in the impulse response of each channel (transmitter-receiver pair) is no longer a Gaussian random variable with zero mean but a Gaussian random variable with non-zero mean (which depends on the Rician factor). All other taps are still modeled as Gaussian random variables with zero mean. We further assume that the variances of all taps are the same.

Figure 5.21 and Figure 5.22 present the average MSE of each tap in the system in the colored and white noise environments, respectively. Figure 5.23 and Figure 5.24 illustrate the average MSE of elements of $\mathbf{\Sigma}$ in the colored and white noise environments, respectively. Again, the exponentially decreasing trend is observed for both noise environments.

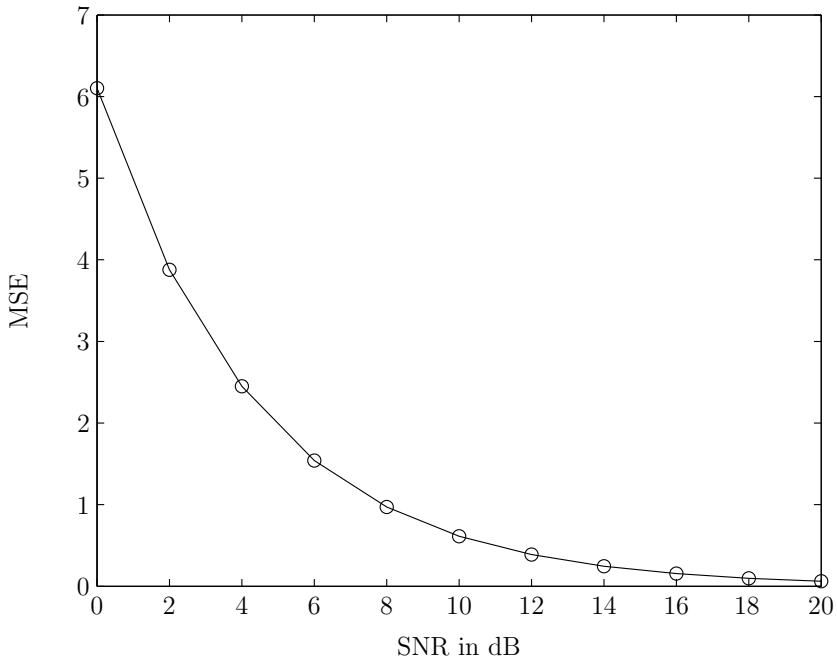

Figure 5.21: Average MSE of each channel taps. There exists LOS paths with Rician factor of 5, in the colored noise environment.

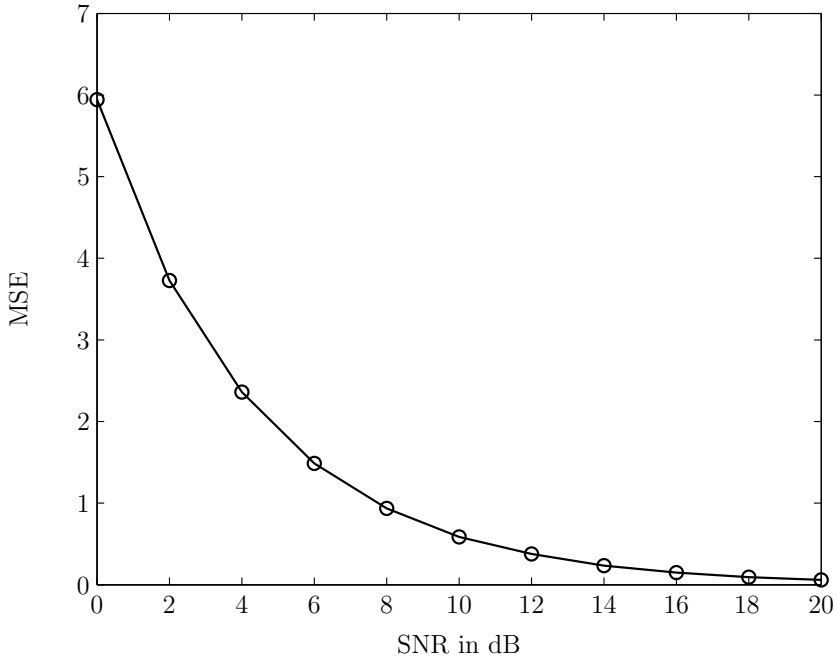

Figure 5.22: Average MSE of each channel taps. There exists LOS paths with Rician factor of 5, in the white noise environment.

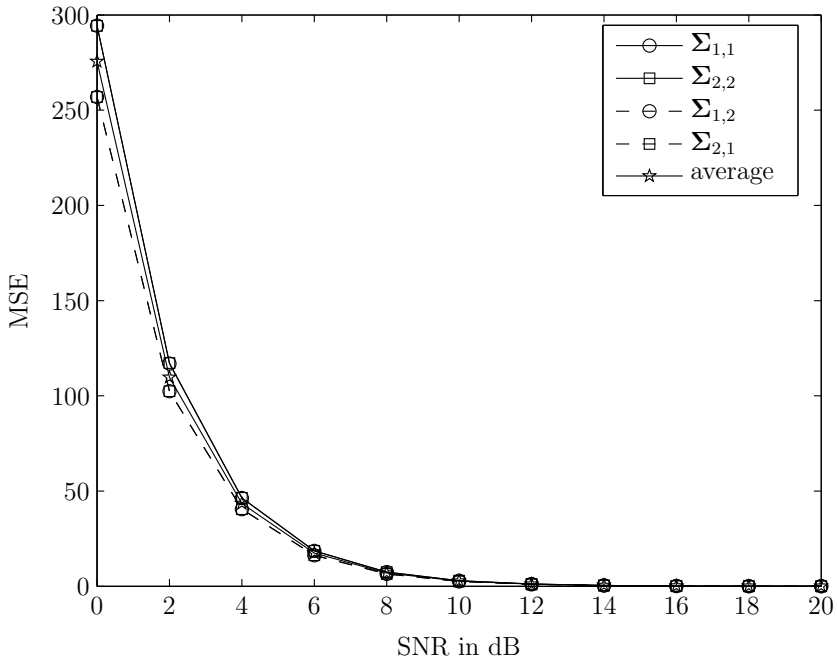

Figure 5.23: Average MSE of elements of $\mathbf{\Sigma}$. There exists LOS paths with Rician factor of 5, in the colored noise environment.

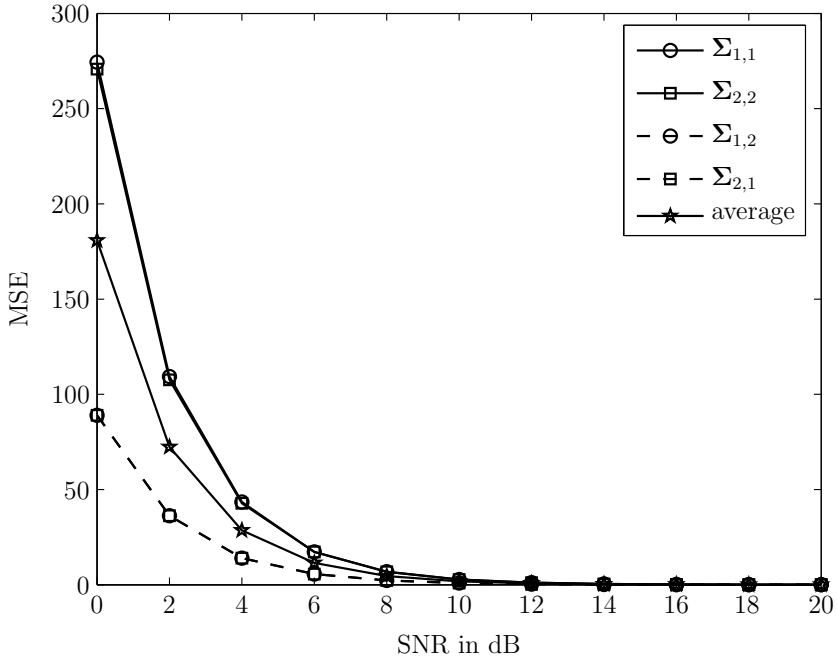

Figure 5.24: Average MSE of elements of $\mathbf{\Sigma}$. There exists LOS paths with Rician factor of 5, in the white noise environment.

Figure 5.25 and Figure 5.26 present the BER of a system with $N = 44,\ M = 4$ and each channel from the transmitter to the receiver has a LOS path, which has the Rician factor of $K = 5$, working in the colored and white noise environments.

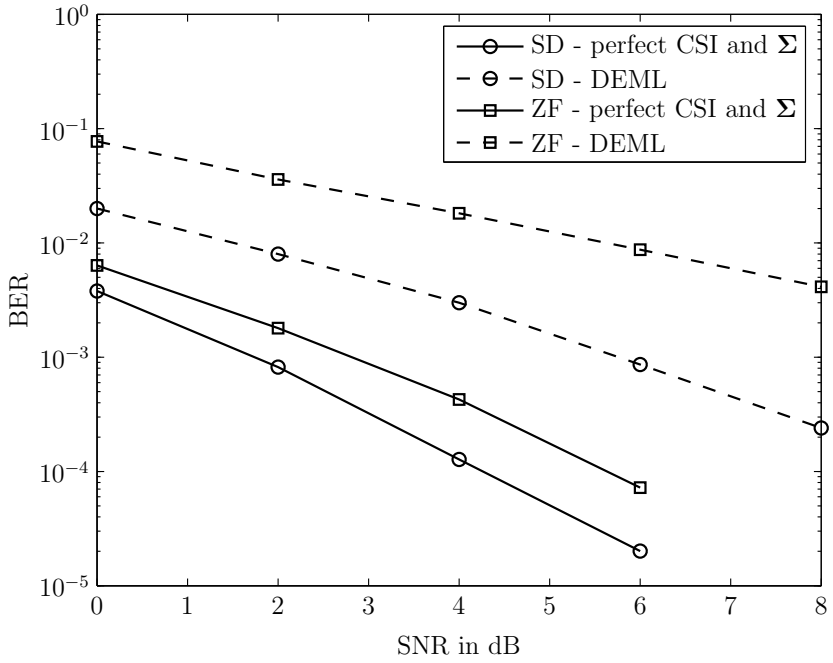

Figure 5.25: BER v.s. SNR for $N = 44, M = 4$, with LOS paths, in the colored noise environment.

With LOS path, the performance of SD when using the channel information from DEML estimator is worse than that of ZF with perfect CSI and noise covariance matrix for both noise cases. This can be explained by examining Figure 5.27 and Figure 5.28 to reveals that the average MSE for the case with LOS path is greater than that for the case without LOS paths for both the channel estimates and noise covariance estimates in the colored noise environment. For the white noise environment, the comparison is illustrated in Figure 5.29 and Figure 5.30.

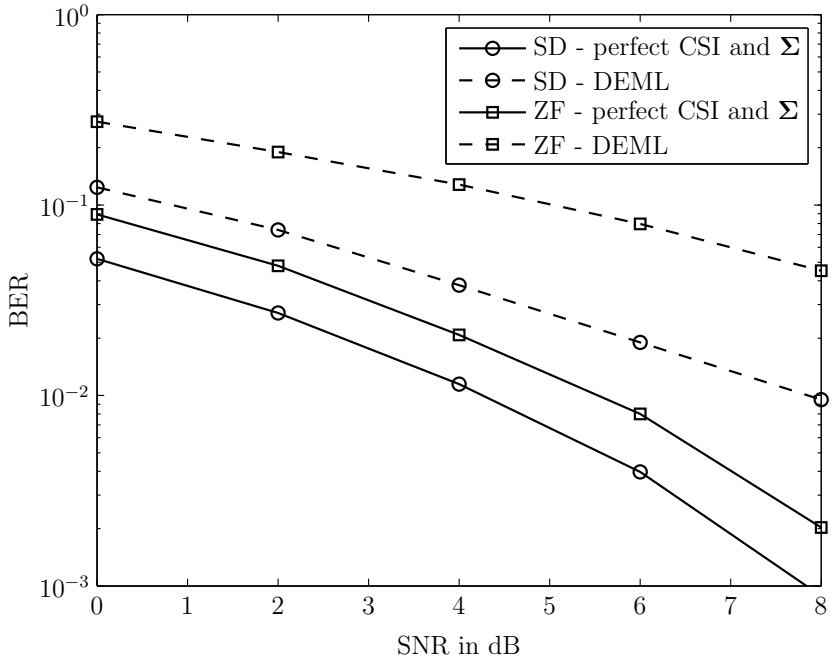

Figure 5.26: BER v.s. SNR for $N = 44, M = 4$, with LOS paths, in the white noise environment.

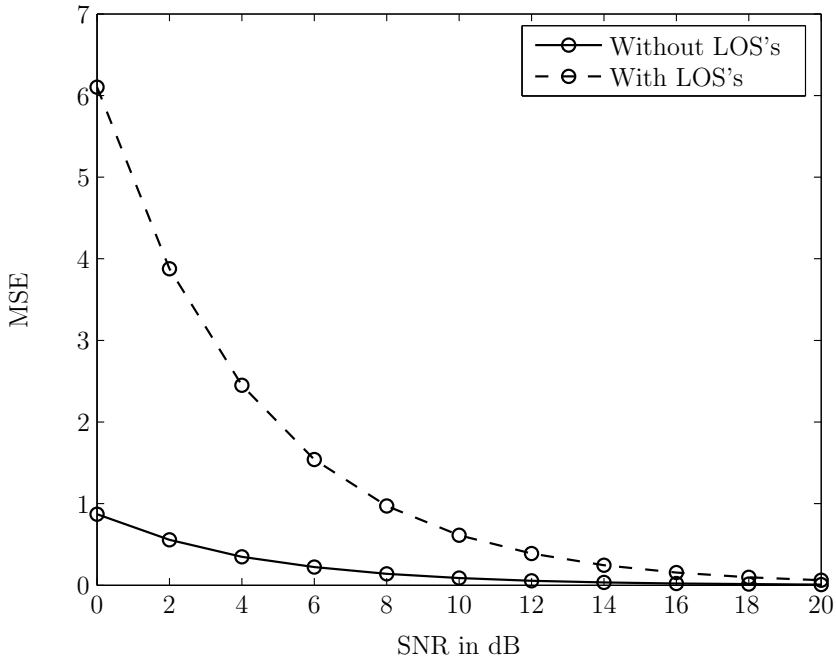

Figure 5.27: Average MSE of each channel tap, with and without LOS paths, in the colored noise environment.

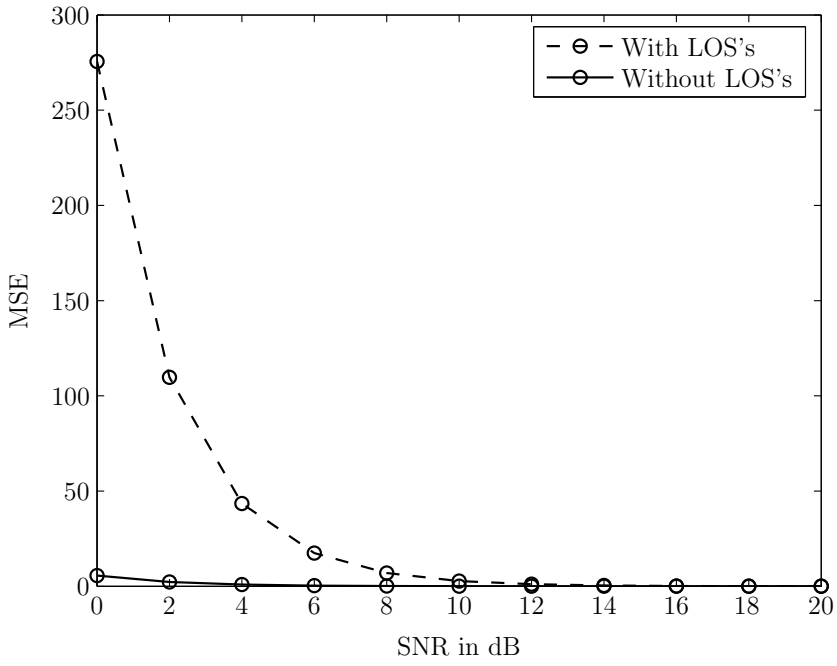

Figure 5.28: Average MSE of elements of $\mathbf{\Sigma}$, with and without LOS paths, in the colored noise environment.

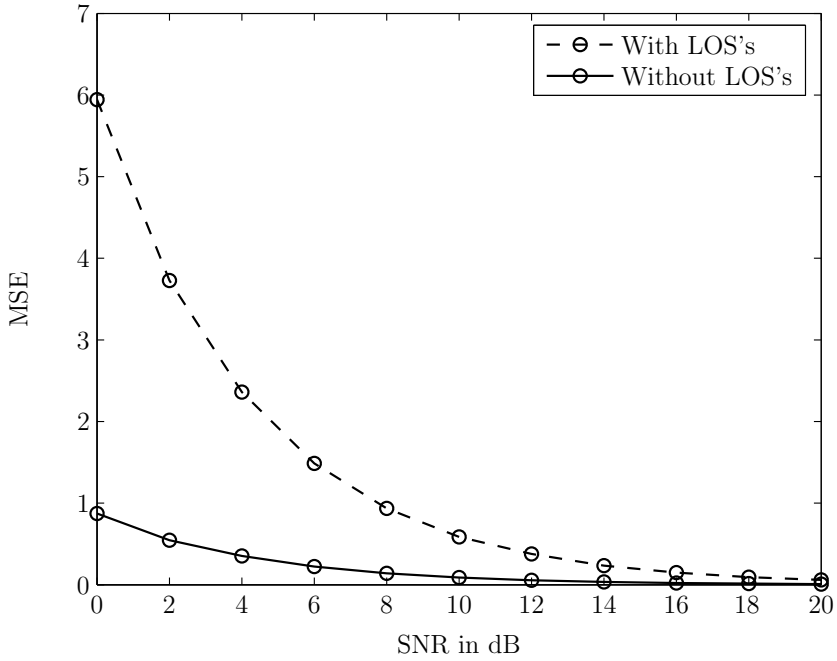

Figure 5.29: Average MSE of each channel tap, with and without LOS paths, in the white noise environment.

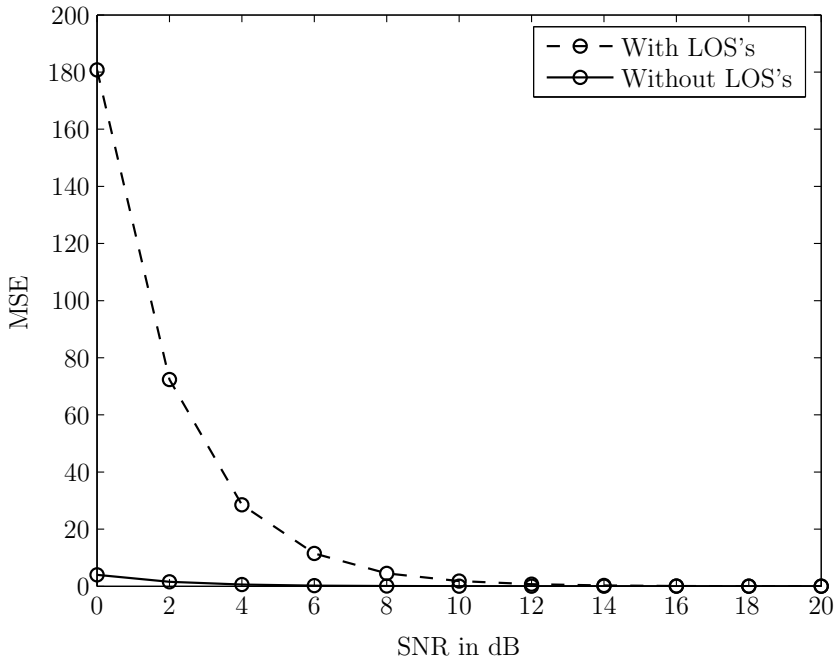

Figure 5.30: Average MSE of elements of $\mathbf{\Sigma}$, with and without LOS paths, in the white noise environment.

Figure 5.31 gives us the performance for two cases: $N = 44,\ M = 4$ and $N = 24,\ M = 4$ in which the system works under the colored noise environment. Figure 5.32 presents the performance of the same system under the white noise environment. We see that for both noise cases, the performance of frame of longer data symbols is again better than that of frame of shorter data symbols.

In Figure 5.33, the BER for the system with $N = 44$ and $M = 4$ working under the colored and white noise environments is presented. Similar to the case of no LOS path in the system, the performance in the colored noise environment outperforms that of the white noise environment.

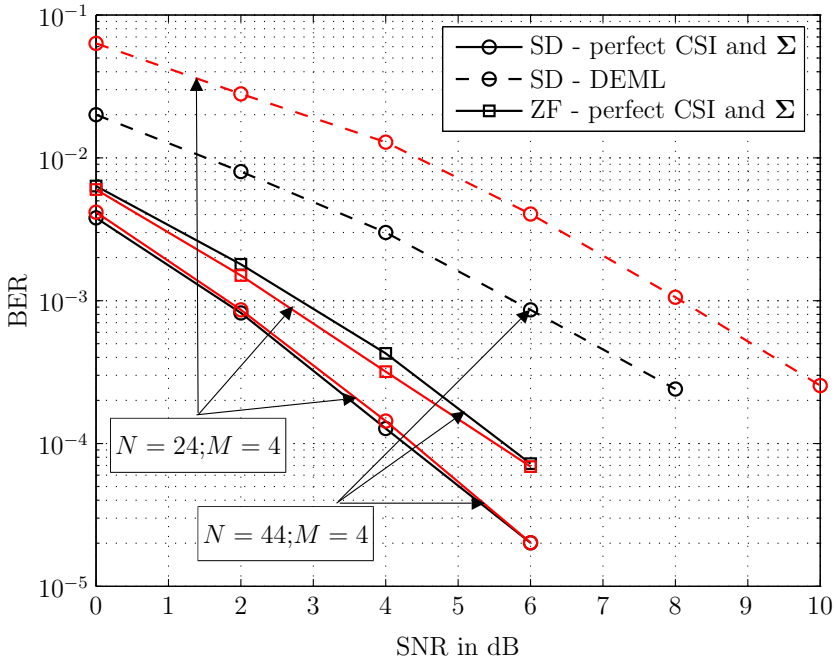

Figure 5.31: BER v.s. SNR for $N = 44, M = 4$ and $N = 24, M = 4$, with LOS paths, in the colored noise environment.

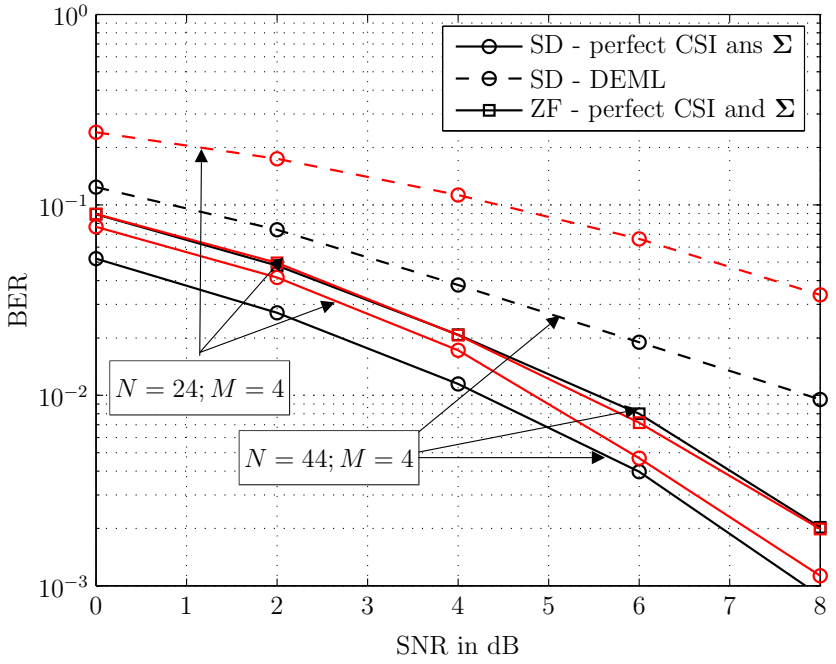

Figure 5.32: BER v.s. SNR for $N = 44, M = 4$ and $N = 24, M = 4$, with LOS paths, in the white noise environment.

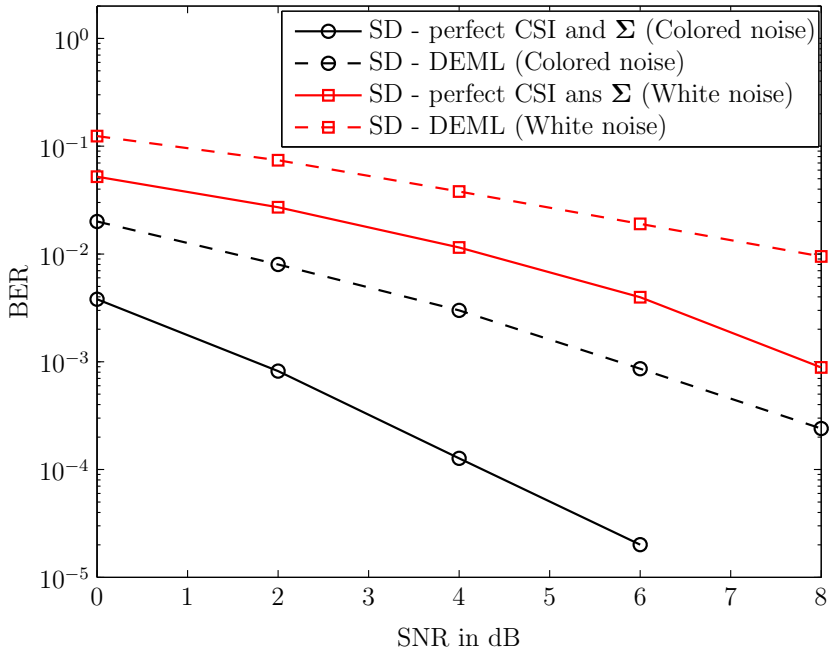

Figure 5.33: BER v.s. SNR for $N = 44, M = 4$, with LOS paths, in the colored and white noise environment.

5.3 Flat fast fading channels

We now consider the scenario in which the channel from each transmitter-receiver pair changes from symbol to symbol (fast fading channels). Here, we adopt the Jake's model in [26]. Our system has $N_i = 1$ transmitter and $N_0 = 2$ receivers. The channels from the transmitter to receivers has $f_{max}T = 0.01,\ 0.005,\ 0.0005$ where f_{max} is the maximum Doppler shift and T is the symbol period. For each value of $f_{max}T$, we consider the frames that have length of $N = 14,\ 24,\ 44,\ 64$ in which the $M = 4$ first symbols are used as pilot symbols. We make an assumption (not true in practice) that, during the training symbols, the channels fluctuate negligibly so that we consider it as unchanged. We apply the DEML algorithm to estimates the channel information. We further assume that the obtained information is unchanged during the data symbols. It is noticed that the above assumptions is violated in case of large value of $f_{max}T$ or in case of long frame. Figure 5.34 and 5.35 show the BER performance for our approach in fast fading channels in the colored noise and white noise environments, respectively.

As observed, the smaller the value of $f_{max}T$ and frame length are, the better the performance is. For $f_{max}T = 0.0005$ and for the case that number of pilot symbols is around 10% of frame length, the performance of SD using DEML algorithm is quite near that of SD with perfect CSI.

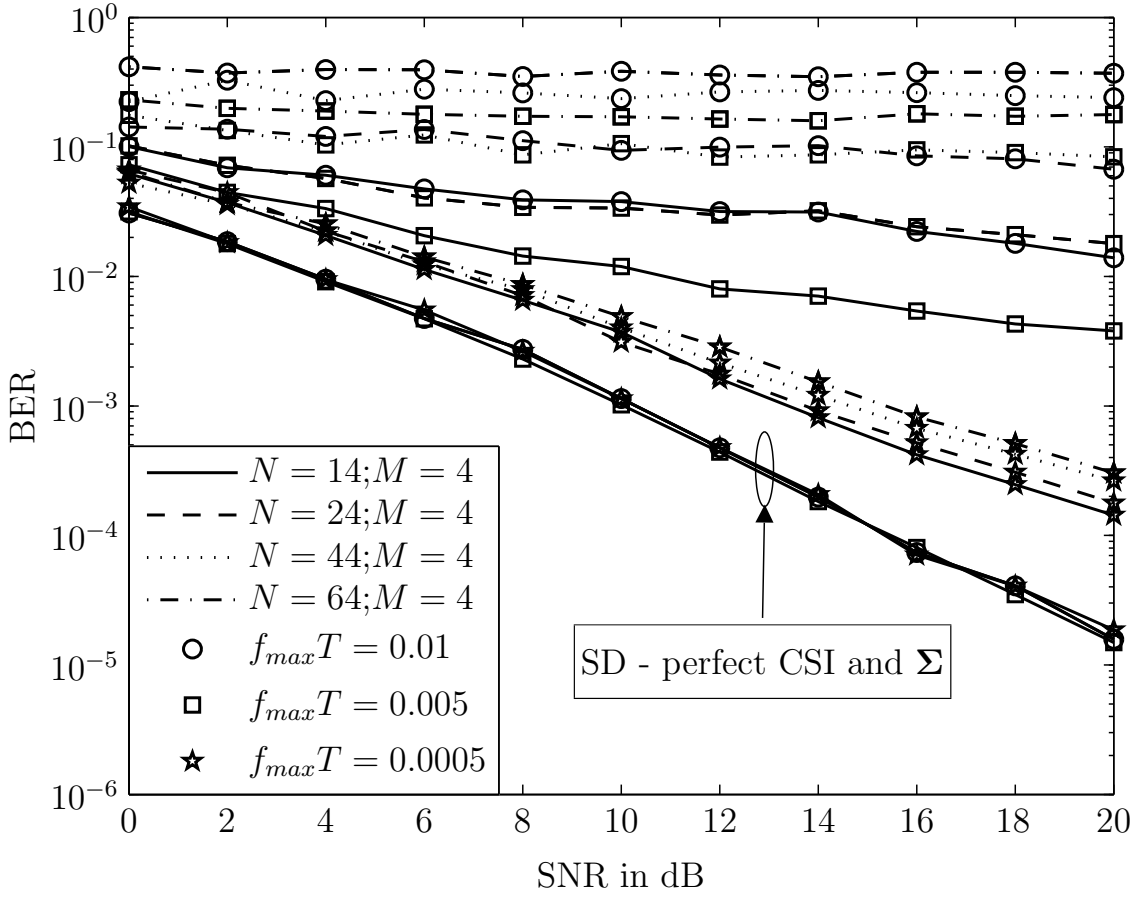

Figure 5.34: BER v.s. SNR for fast fading channels in colored noise environment

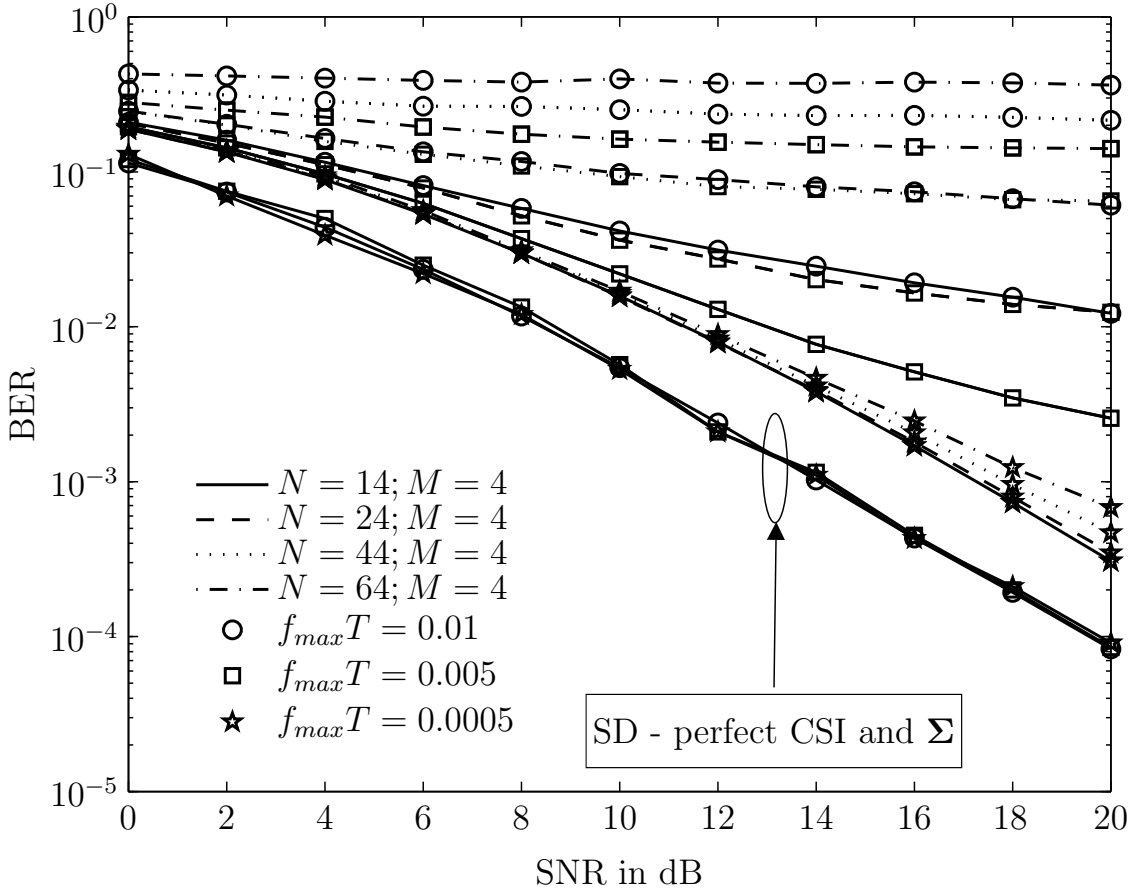

Figure 5.35: BER v.s. SNR for fast fading channels in white noise environment.

CHAPTER 6

CONCLUSION AND RECOMMENDATION

6.1 Conclusion

Prior to the discussion of channel estimation and detection for MIMO systems, we developed the discrete-time model for fading MIMO systems which is used throughout the dissertation to examine the performance of our proposed channel estimation and signal decoding algorithms.

The problem of finding closest lattice point is presented for infinite lattice. From this, the Sphere Decoder which is applied in communication problems are presented.

Next, we propose the decouple maximum likelihood (DEML) estimator for estimating the channel coefficients of MIMO systems as well as the noise covariance matrix at the receivers. The estimated parameters are used in the detection which employs the Sphere Decoding algorithm.

The simulation results are given to illustrate the performance of the proposed method. The method can be applied in MIMO quasi-static flat fading systems, quasi-static frequency-selective fading systems. It also give reasonable results for MIMO fast-fading systems.

6.2 Recommendation

In this dissertation, our research is all based on QPSK signalling, it will be interesting to investigate our approach's performance with other signal constellations such as 16-QAM or 64-QAM. It would be also interesting and challenging to investigate the structure of pilot symbols in order to have the most accurate

channel information. Furthermore, with the development of space-time code [28], it is of interest to investigate our proposed approach with coded MIMO systems.

BIBLIOGRAPHY

[1] L. C. Godara, "Application of antenna arrays to mobile communications, part i: Performance improvement, feasibility, and system considerations," *Proceedings of the IEEE*, no. 87, pp. 1031–1060, 1997.

[2] L. C. Godara, "Application of antenna arrays to mobile communications, part ii: Beam-forming and direction-of-arrival considerations," *Proceedings of the IEEE*, pp. 1195–1245, Aug. 1997.

[3] J. C. Liberti and T. S. Rappaport, *Smart Antennas for Wireless Communications: IS-95 and Third Generation CDMA Applications*. Prentice Hall, 1999.

[4] A. Lozano, F. R. Farrokhi, and R. A. Valenzuela, "Lifting the limits on high-speed wireless data access using antenna arrays," *IEEE Commun. Mag.*, pp. 156–162, 2001.

[5] R. D. Murch and K. B. Letaief, "Antenna systems for broadband wireless access," *IEEE Commun. Mag.*, pp. 76–83, Apr. 2002.

[6] G. J. Foschini and M. J. Gans, "On the limits of wireless communications in a fading environment when using multiple antennas," *Wireless Personal Commun.*, pp. 315–335, 1998.

[7] M. Viberg, P. Stoice, and B. Ottersten, "Maximum likelihood array processing in spatially correlated noise fields using parameterized signals," *IEEE Trans. Signal Processing*, vol. 45, pp. 996–1004, Apr 1997.

[8] A. Dogandzic, W. Mo, and Z. Wang, "Semi-blind simo flat-fading channel estimation in unknown spatially correlated noise using the em algorithm," *IEEE Trans. Signal Processing*, vol. 52, pp. 1791–1797, Jun 2004.

[9] J. H. Conway and N. J. Sloane, *Sphere Packing, Lattices and Groups*. New York: Springer-Verlag, 3 ed., 1998.

[10] E. Viterbo and E. Biglieri, "A universal lattice decoder," *GRETSI 14-eme Colloque, Juan-les-Pins, France*, Sept. 2000.

[11] E. Viterbo and J. Boutros, "A universal lattice decoder for fading channels," *IEEE Transactions on Information Theory*, vol. 45, pp. 1639–1642, 1999.

[12] M. O. Damen, A. Chkeif, and J. C. Belfiore, "Lattice code decoder for space-time codes," *IEEE Communications Letters*, pp. 161–163, May 2000.

[13] A. Agrell, T. Eriksson, A. Vardy, and K. Zeger, "Closest point search in lattices," *IEEE Transactions on Information Theory*, vol. 48, no. 8, pp. 2201–2214, 2002.

[14] M. O. Damen, H. E. Gamal, and G. Caire, "On Maximum-Likelihood detection and the search for the closest lattice point," *IEEE Transactions on Information Theory*, vol. 49, Oct. 2003.

[15] L. Brunel and J. Boutros, "Lattice decoding for joint detection in direct sequence cdma systems," *IEEE Transactions on Information Theory*, vol. 49, pp. 1030–1037, April 2000.

[16] B. M. Hochwald and S. Brink, "Achieving near-capacity on a multiple-antenna channels," *IEEE Transactions on Communications*, vol. 51, pp. 389–399, 2003.

[17] A. Windpassinger and R. Fischer, "Low-complexity near maximum likelihood detection and precoding for mimo systems using lattice reduction," *Proc. IEEE Information Theory Workshop Paris, France*, pp. 345–348, Apr 2003.

[18] J. Li, B. Halder, P. Stoica, and M. Viberg, "Computationally efficient angle estimation for signals with known waveforms," *Acoustics, Speech, and Signal Processing, IEEE Transactions on*, pp. 2154–2163, Sep 1995.

[19] T. S. Rappaport, *Wireless Communications: Principles and Practice*. Prentice Hall, 2 ed., 2002.

[20] J. Proakis, *Digital Communications*. New York: McGraw-Hill, 4 ed., 2000.

[21] Z. Wang and G. B. Giannskis, "Wireless multicarrier communications," *IEEE Signal Processing Magazine*, pp. 29–48, May 2000.

[22] M. Ajtai, "The shortest vector problem in L_2 in NP-hard for randomized reductions," *Proceedings of the 30th Annual ACM Symposium on Theory of Computing*, pp. 10–19, 1998.

[23] M. Pohst, "On the computation of lattice vectors of minimal length, successive minima and reduced basis with application," *ACM SIGSAM*, vol. 15, pp. 37–44, 1981.

[24] G. G. Golub and C. F. Van Loan, *Matrix Computations*. McGraw-Hill:New York, 3 ed., 1995.

[25] T. Soderstrom and P. Stoica, *System Identification*. London: Prentice Hall, 1989.

[26] W. C. Jakes, *Microwave Mobile Communications*. Piscataway, NJ: IEEE Press, 1994.

[27] J. R. Barry, E. A. Lee, and D. G. Messerschmitt, *Digital Communication*. Kluwer Academic Publishers, 3 ed., 2003.

[28] S. M. Alamouti, "A simple tranmitter diversity scheme for wireless communications," *IEEE Journal of Select. Areas Commum.*, vol. 16, pp. 1451–1458, Oct 1998.